nagra.

Arbeitsbericht NAB 22-02

TBO Stadel-2-1: Data Report

Dossier X
Petrophysical Log Analysis

September 2022

S. Marnat & J.K. Becker

National Cooperative
for the Disposal of
Radioactive Waste

Hardstrasse 73
P.O. Box
5430 Wettingen
Switzerland
Tel. +41 56 437 11 11

nagra.ch

nagra.

Arbeitsbericht NAB 22-02

TBO Stadel-2-1: Data Report

Dossier X
Petrophysical Log Analysis

September 2022

S. Marnat[1] & J.K. Becker[2]

[1] Ad Terra Energyl
[2] Nagra

Keywords:
STA2-1, Nördlich Lägern, TBO, deep drilling campaign, stochastic log interpretation, MultiMin analyses, petrophysical logs, lab data, Multi-Sensor Core Logger, MSCL, mineralogy, clay content, clay typing, porosity

National Cooperative for the Disposal of Radioactive Waste

Hardstrasse 73
P.O. Box
5430 Wettingen
Switzerland
Tel. +41 56 437 11 11

nagra.ch

Nagra Arbeitsberichte ("Working Reports") present the results of work in progress that have not necessarily been subject to a comprehensive review. They are intended to provide rapid dissemination of current information.

This NAB aims at reporting drilling results at an early stage. Additional borehole-specific data will be published elsewhere.

In the event of inconsistencies between dossiers of this NAB, the dossier addressing the specific topic takes priority. In the event of discrepancies between Nagra reports, the chronologically later report is generally considered to be correct. Data sets and interpretations laid out in this NAB may be revised in subsequent reports. The reasoning leading to these revisions will be detailed there.

This report was finalised in June 2023.

This Dossier was prepared by a project team consisting of:
S. Marnat (data analyses, interpretation and writing)
J.K. Becker (project administration and writing)

Editorial work: P. Blaser and M. Unger

The Dossier has greatly benefitted from technical discussions with, and reviews by, internal experts. Their input and work are very much appreciated.

Table of Contents

Table of Contents I

List of Tables II

List of Figures II

List of Appendices III

List of Plates III

Abbreviations IV

1 Introduction 1
1.1 Context 1
1.2 Location and specifications of the borehole 2
1.3 Documentation structure for the STA2-1 borehole 6
1.4 Scope and objectives of this dossier 7

2 Data preparation 9
2.1 Used log data 9
2.2 Used core data 14
2.3 Multi-sensor Core Logger (MSCL) data 14
2.4 MultiMin input dataset preparation 16
2.5 Preliminary calculations (Precalc) 17

3 Petrophysical log interpretation 19
3.1 MultiMin interpretation 19
3.2 Bad hole treatment and quality of results 22
3.2.1 Indicator for input data quality (LQC_INDEX) 22
3.2.2 Indicator for the mathematical model (CONDNUM and NFUN) 22
3.2.3 Indicator for the MultiMin interpretation results (MULT_QC and QUALITY) 23

4 Results of the calibrated stochastic log interpretation 25
4.1 Comparison of interpretation results with core data 25
4.2 Main results of the core-calibrated log analyses in the STA2-1 borehole 33
4.3 Main results of the core-calibrated log analysis in the Opalinus Clay (800.67 – 906.87 m) 37

5 Summary 47

6 References 49

List of Tables

Tab. 1-1: General information about the STA2-1 borehole 2
Tab. 1-2: Core and log depth for the main lithostratigraphic boundaries in the STA2-1 borehole..... 5
Tab. 1-3: List of dossiers included in NAB 22-02 6
Tab. 3-1: List of MultiMin models used in STA2-1 20

List of Figures

Fig. 1-1: Tectonic overview map with the three siting regions under investigation 1
Fig. 1-2: Overview map of the investigation area in the Nördlich Lägern siting region with the location of the STA2-1 borehole in relation to the boreholes Weiach-1, BUL1-1, STA3-1 and BAC1-1 3
Fig. 1-3: Lithostratigraphic profile and casing scheme for the STA2-1 borehole..... 4
Fig. 2-1: HNGS HFK versus ECS DWK_ALKNA in INT2A..... 10
Fig. 2-2: HNGS HFK versus ECS DWK_ALKNA in INT3..... 11
Fig. 2-3: Petrophysical log availability and short gaps in the STA2-1 borehole 13
Fig. 2-4: XRF (black dots) and ECS WALK2 (red curves) elements comparison for STA2-1..... 15
Fig. 2-5: Core (black dots: spectral gamma ray, blue dots XRF thorium) and wireline HNGS (red curves) spectral gamma ray elements comparison 16
Fig. 4-1: Weight-% of dry clay (y-axis) compared to core XRD data (x-axis), Villigen to Schinznach Formation)..... 26
Fig. 4-2: Weight-% of non-potassic dry clay (y-axis) compared to core XRD data (x-axis), Villigen to Klettgau Formation 27
Fig. 4-3: Weight-% of illite (x-axis) compared to core XRD data (y-axis), Villigen to Klettgau Formation..... 28
Fig. 4-4: Weight-% of QF-silicates (y-axis) compared to core XRD data (x-axis), Villigen to Schinznach Formation 29
Fig. 4-5: Weight-% of carbonates (y-axis) compared to core XRD data (x-axis), Villigen to Schinznach Formation 30
Fig. 4-6: Weight-% of dolomite (y-axis) compared to core XRD data (x-axis), Villigen to Schinznach Formation 31
Fig. 4-7: Total porosity (v/v, y-axis) compared to core data (x-axis), «Felsenkalke» + «Massenkalk» to Schinznach Formation 32
Fig. 4-8: Dry clay weight percentage frequency histogram in the Opalinus Clay..... 38
Fig. 4-9: Dry clay weight percentage frequency histogram in the upper section of the Opalinus Clay (above 864.7 m) 39
Fig. 4-10: Dry clay weight percentage frequency histogram in the lower section of the Opalinus Clay (below 864.7 m)..... 40

Fig. 4-11: Calcite weight percentage frequency histogram in the Opalinus Clay 41
Fig. 4-12: Siderite weight percentage frequency histogram in the Opalinus Clay 42
Fig. 4-13: QF-silicates (quartz and feldspars) weight percentage frequency histogram in the Opalinus Clay 43
Fig. 4-14: Total porosity frequency histogram in the Opalinus Clay 44
Fig. 4-15: Main log and core results in the Opalinus Clay 45

List of Appendices

App. A: Precalc parameters table
App. B: List of MultiMin models
App. C: Parameters used in the different MultiMin models

List of Plates

Plate 1: Comparison of calculated log curves and measured petrophysical log curves
Plate 2: Results of the core-calibrated petrophysical log interpretation

Note: In the digital version of this report the appendices and plates can be found under the paper clip symbol.

Abbreviations

ANHYDR	Anhydrite weight percentage from MultiMin
APLC	Corrected neutron hydrogen index from APS (limestone matrix)
APLC_PRED	APLC prediction by MultiMin
APS	Accelerator Porosity Sonde
B/E	Barns/Electron
BS	Drilling / Coring Bit Size
CALCITE	Calcite weight percentage from MultiMin
CALI	Caliper
CARBONATES	Carbonates weight percentage from MultiMin
CHLORITE	Chlorite weight percentage from MultiMin
COAL	Coal weight percentage from MultiMin
COMPOSITE	Composite log, validated logs dataset
CONDNUM	MultiMin model condition number
CT	Conductivity in the formation
CT_PRED	CT prediction by MultiMin
CU	Capture Unit, unit for sigma
CXO	Conductivity in the invaded zone
CXO_PRED	CXO prediction by MultiMin
DENS	Bulk density
DOLOMITE	Dolomite weight percentage from MultiMin
DRHO	Bulk density correction
DRY_CLAY	Dry clay weight percentage from MultiMin
dRRC	Rush raw corrected data
DTCO	Compressional wave slowness from far monopole mid frequency source compressional wave slowness
DTCO_PRED	DTCO prediction by MultiMin
DTSM	Shear wave slowness from inline X-Dipole (90°) source
DTSM_PRED	DTSM prediction by MultiMin
DWAL_ALKNA	Dry weight fraction aluminium, ECS ALKNA closure model
DWAL_MGWALK	Dry weight fraction aluminium, ECS MGWALK closure model
DWAL_WALK2	Dry weight fraction aluminium, ECS WALK2 closure model

DWCA_MGWALK	Dry weight fraction calcium, ECS MGWALK closure model
DWCA_WALK2	Dry weight fraction calcium, ECS WALK2 closure model
DWFE_CORR	Dry weight fraction iron, calibrated to XRF iron content
DWFE_MGWALK	Dry weight fraction iron, ECS MGWALK closure model
DWFE_WALK2	Dry weight fraction iron, ECS WALK2 closure model
DWK_ALKNA	Dry weight fraction potassium, ECS ALKNA closure model
DWK_MGWALK	Dry weight fraction potassium, ECS MGWALK closure model
DWMG_MGWALK	Dry weight fraction magnesium, ECS MGWALK closure model
DWSI_MGWALK	Dry weight fraction silicon, ECS MGWALK closure model
DWSI_WALK2	Dry weight fraction silicon, ECS WALK2 closure model
DWSU_MGWALK	Dry weight fraction sulphur, ECS MGWALK closure model
DWSU_WALK2	Dry weight fraction sulphur, ECS WALK2 closure model
DWTI_MGWALK	Dry weight fraction titanium, ECS MGWALK closure model
DWTI_WALK2	Dry weight fraction titanium from ECS, ECS WALK2 closure model
ECS	Elemental Capture Spectroscopy
EDTC	Enhanced Digital Telemetry Cartridge
EMS	Environment Measurement Sonde
FE_MIN	Iron-rich minerals (Siderite, pyrite, iron oxides)
FLAG_BADHOLE_DN	Badhole flag from the Density-Neutron crossplot
FLAG_BADHOLE_OVERGAUGE	Badhole flag from the Caliper
FLAG_BADHOLE_RUGO	Badhole flag from the Density correction
FLAG_BADHOLE_STOF	Badhole flag from the Neutron stand-off
FMI	Fullbore Formation Microimager
g/cm^3	Gram per cubic centimetre
GAPI	Unit of radioactivity used for natural Gamma Ray logs
GEOLOG	Emerson software used for log interpretation
GPIT	General Purpose Inclinometry Tool

GR	Total Gamma Ray
GR_KCOR	Total Gamma Ray corrected for mud potassium
GR_KCOR_PRED	GR_KCOR prediction by MultiMin
HAEMATITE	Haematite weight percentage from MultiMin
HALITE	Halite weight percentage from MultiMin
HDAR	Hole diameter from area
HDRA	Bulk density correction
HFK	Potassium concentration from HNGS
HI	Hydrogen Index
HNGS	Hostile Natural Gamma Ray Sonde
HRLT	High Resolution Laterolog array Tool
HSGR	HNGS Standard Gamma Ray
HTHO	Thorium concentration from HNGS
HURA	Uranium concentration from HNGS
HURA_PRED	HURA prediction by MultiMin
ILLITE	Illite weight percentage from MultiMin
KAOLIN	Kaolinite weight percentage from MultiMin
KEROGEN	Kerogen weight percentage from MultiMin
LEH.QT	Logging Equipment Head with Tension
LQC_INDEX	Log Quality Control Index
MCFL	Micro-Cylindrical Focused Log
MHF	Micro Hydraulic Fracturing
MSCL	Multi-Sensor Core Logger
MULT_QC	MultiMin analysis quality flag
MULTIMIN	Multi mineral and multi fluid analysis module in Geolog software
m MD	Metre measured depth
MSIP	Modular Sonic Imaging Platform
NFUN	Number of MultiMin iterations
NO_K_CLAYS	Non-potassic clays weight percentage from MultiMin
ORTHOCL	K-Feldspars weight percentage from MultiMin
p.u.	Porosity unit
PEFZ	Photoelectric factor
PEFZ_PRED	PEFZ prediction by MultiMin
PHI_PICNO	Core pycnometer porosity

PHI_WL1	Core water-loss porosity (105 °C) using bulk wet density
PHI_WL2	Core water-loss porosity (105 °C) using grain density
PHIE	Effective porosity
PHIT	Total porosity
PLAGIO	Plagioclases weight percentage from MultiMin
PPC	Power positioning device and caliper tool
PRECALC	Precalculation module in the Geolog software
PYRITE	Pyrite weight percentage from MultiMin
QC	Quality Control
QF_SILICATES	Matrix quartz and feldspars weight percentage from MultiMin
QUALITY	MultiMin analysis quality
QUARTZ	Quartz weight percentage from MultiMin
RCL	Reduced Composite Log
RHGE_WALK2	Matrix density from elemental concentrations (WALK2 model)
RHOB_CALC	Bulk density computed from core data
RHOG	Grain density from MultiMin
RHOS	Solids density
RHOZ	Bulk density
RHOZ_PRED	RHOZ prediction by MultiMin
RT_HRLT	HRLT true formation resistivity
RUGO	Borehole wall rugosity
RXOZ	Invaded formation resistivity filtered at 18 inches
SIDER	Siderite weight percentage from multimin
SIGF	Macroscopic cross section for the absorption of thermal neutrons, or capture cross section, of a volume of matter, measured in capture units [c.u.]
SIGF_PRED	SIGF prediction by MultiMin
SLB	Abbreviation for Schlumberger Logging Company
SP	Spontaneous Potential
STOF	APS Stand-Off
SWE	Effective water saturation
SWT	Total water saturation
TLD	Three-detector Lithology Density
TOC	Total organic carbon [w/w or wt.-%]

U	Photoelectric cross-section computed by Precalc [b/cc]
UBI	Ultrasonic Borehole Imager
v/v	Volume per volume
VCL	Volume of wet clay
VOL_ANHYDR	MultiMin volume of anhydrite
VOL_ANORTH	MultiMin volume of plagioclase
VOL_CALCITE	MultiMin volume of calcite
VOL_CHLOR	MultiMin volume of chlorites
VOL_DOLOM	MultiMin volume of dolomite
VOL_ILLITE	MultiMin volume of illite
VOL_ORTHOCL	MultiMin volume of potassic feldspars
VOL_SIDER	MultiMin volume of siderite
VP	Compressional waves velocity [m/s]
VS	Shear waves velocity [m/s]
VPVS	Compressional and shear waves velocity ratio
VPVS_INPUT	Array Monte-Carlo input for VP/VS
ECS WT.-%	Weight concentration
W/W	Weight per weight, concentration
WANH_WALK2	Dry weight fraction anhydrite/gypsum from ECS (WALK2 model)
WCAR_WALK2	Dry weight fraction carbonate from ECS (WALK2 model)
WCLA_WALK2	Dry weight fraction clay from ECS (WALK2 model)
WEVA_WALK2	Dry weight fraction salt from ECS (WALK2 model)
WPYR_WALK2	Dry weight fraction pyrite from ECS (WALK2 model)
WQFM_WALK2	Dry weight fraction quartz+feldspar+mica from ECS (WALK2 model)
WSID_WALK2	Dry weight fraction siderite from ECS (WALK2 model)
XRD	X-Ray Diffraction
µs/ft	Microsecond per foot (unit for sonic slowness)

1 Introduction

1.1 Context

To provide input for site selection and the safety case for deep geological repositories for radioactive waste, Nagra has drilled a series of deep boreholes ("Tiefbohrungen", TBO) in Northern Switzerland. The aim of the drilling campaign is to characterise the deep underground of the three remaining siting regions located at the edge of the Northern Alpine Molasse Basin (Fig. 1-1).

In this report, we present the results from the Stadel-2-1 borehole.

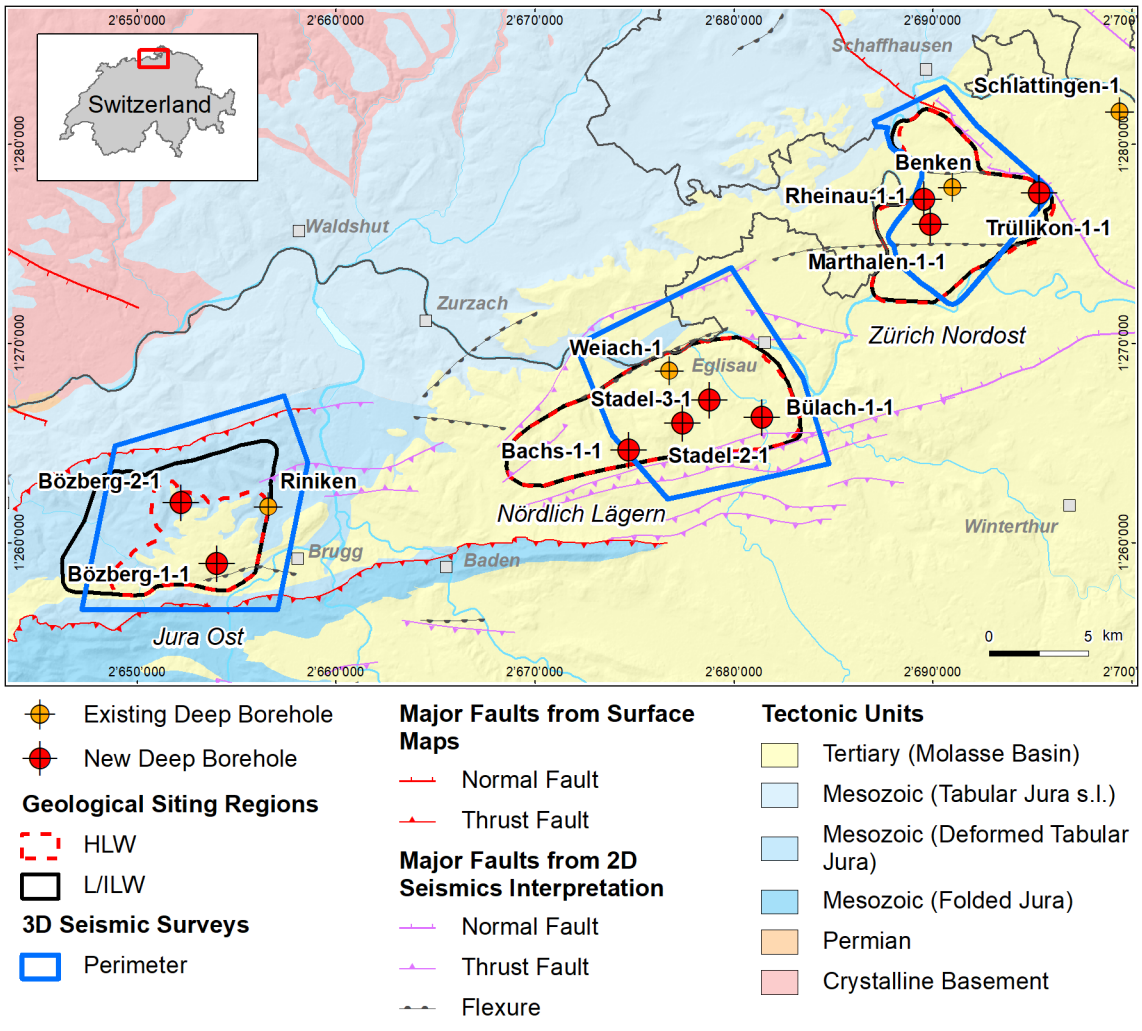

Fig. 1-1: Tectonic overview map with the three siting regions under investigation

1.2 Location and specifications of the borehole

The Stadel-2-1 (STA2-1) exploratory borehole is the seventh borehole drilled within the framework of the TBO project. The drill site is located in the central part of the Nördlich Lägern siting region (Fig. 1-2). The vertical borehole reached a final depth of 1'288.12 m (MD)[1]. The borehole specifications are provided in Tab. 1-1.

Tab. 1-1: General information about the STA2-1 borehole

Siting region	Nördlich Lägern
Municipality	Stadel (Canton Zürich / ZH), Switzerland
Drill site	Stadel-2 (STA2)
Borehole	Stadel-2-1 (STA2-1)
Coordinates	LV95: 2'677'447.617 / 1'265'987.019
Elevation	Ground level = top of rig cellar: 417.977 m above sea level (asl)
Borehole depth	1'288.12 m measured depth (MD) below ground level (bgl)
Drilling period	25th January – 8th July 2021 (spud date to end of rig release)
Drilling company	Daldrup & Söhne AG
Drilling rig	Wirth B 152t
Drilling fluid	Water-based mud with various amounts of different components such as[2]: 0 – 670 m: Bentonite & polymers 670 – 1'051 m: Potassium silicate & polymers 1'051 – 1'117 m: Water & polymers 1'117 – 1'288.12 m: Sodium chloride brine & polymers

The lithostratigraphic profile and the casing scheme are shown in Fig. 1-3. The comparison of the core versus log depth[3] of the main lithostratigraphic boundaries in the STA2-1 borehole is shown in Tab. 1-2.

[1] Measured depth (MD) refers to the position along the borehole trajectory, starting at ground level, which for this borehole is the top of the rig cellar. For a perfectly vertical borehole, MD below ground level (bgl) and true vertical depth (TVD) are the same. In all Dossiers depth refers to MD unless stated otherwise.

[2] For detailed information see Dossier I.

[3] Core depth refers to the depth marked on the drill cores. Log depth results from the depth observed during geophysical wireline logging. Note that the petrophysical logs have not been shifted to core depth, hence log depth differs from core depth.

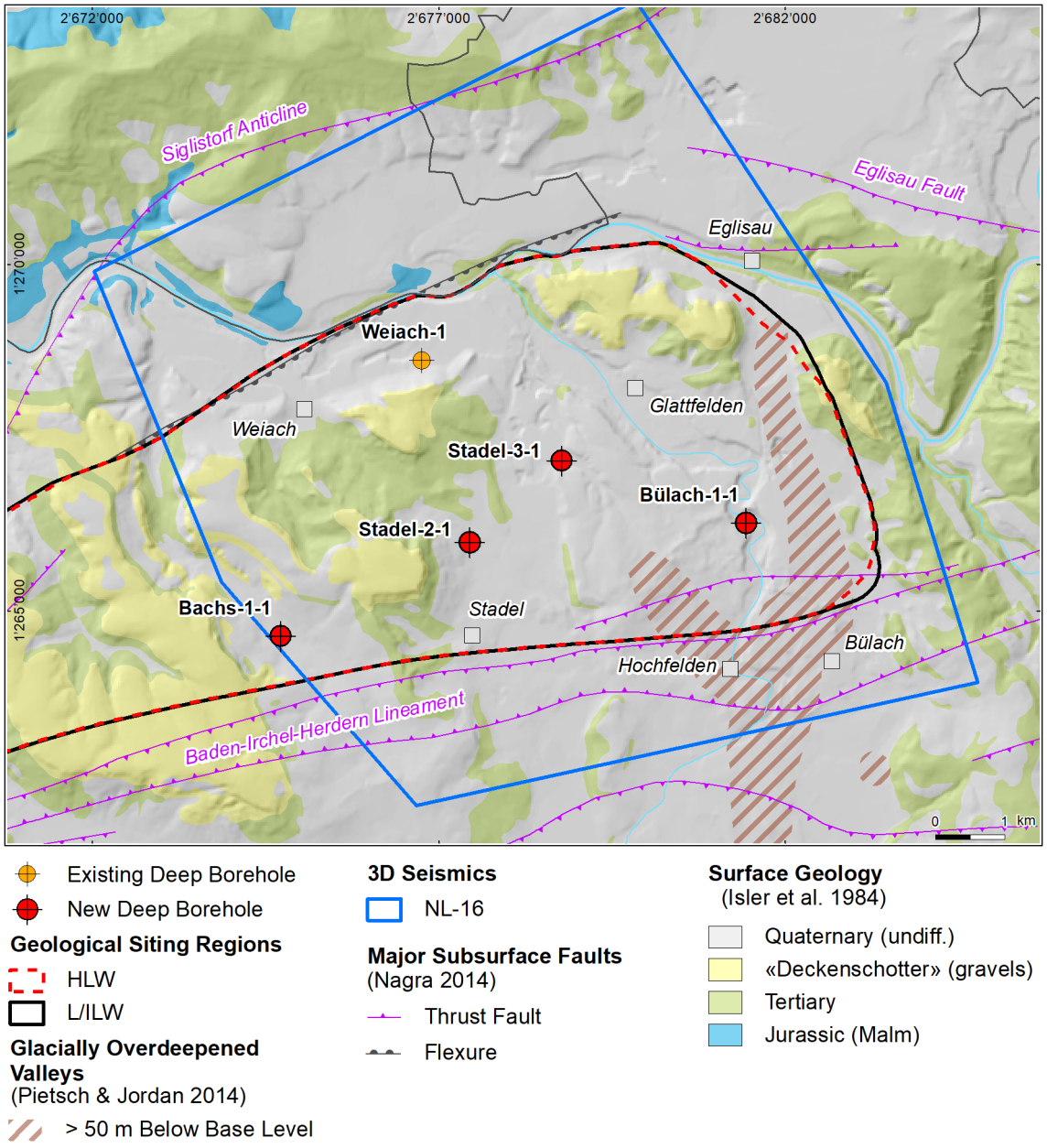

Fig. 1-2: Overview map of the investigation area in the Nördlich Lägern siting region with the location of the STA2-1 borehole in relation to the boreholes Weiach-1, BUL1-1, STA3-1 and BAC1-1

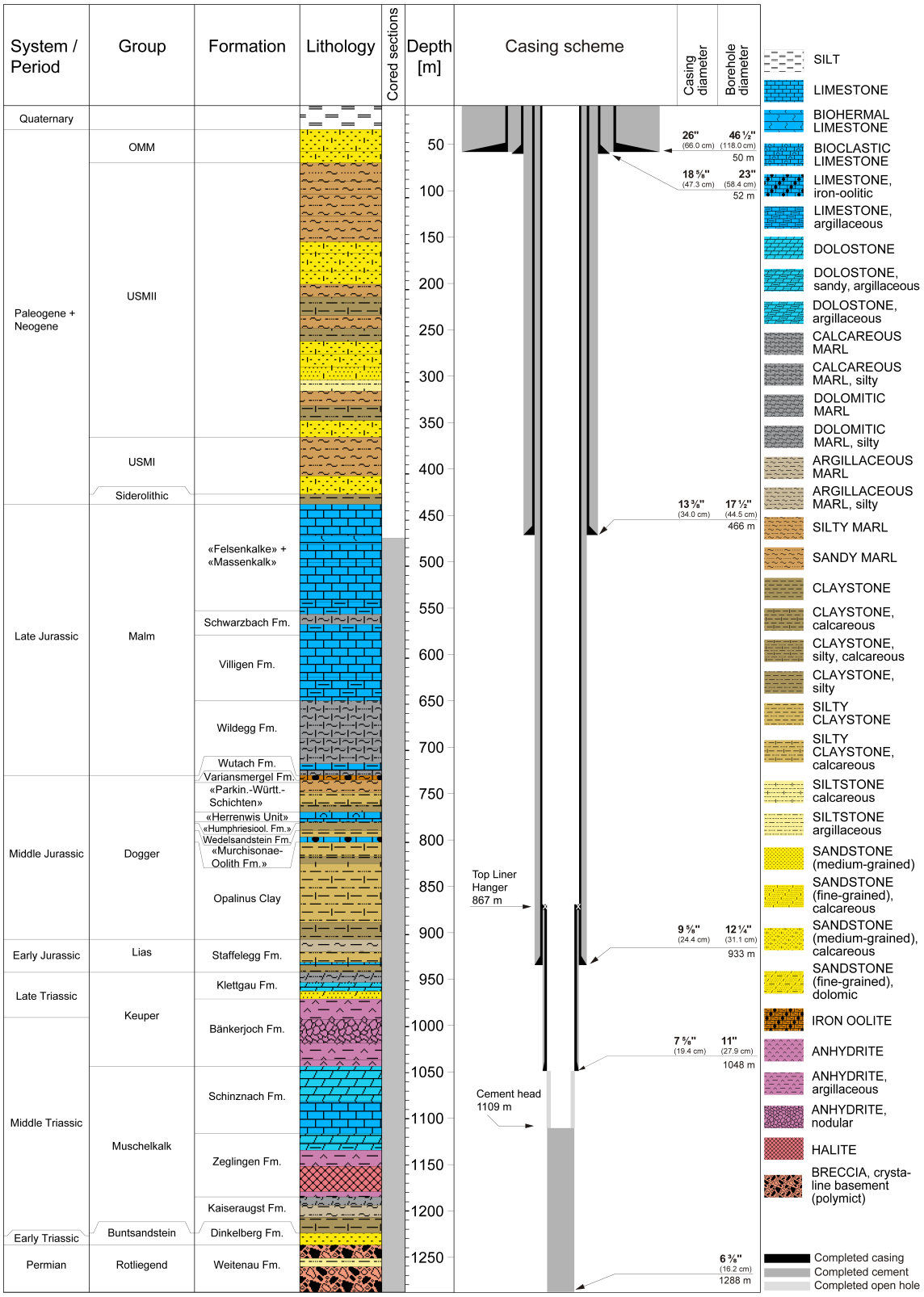

Fig. 1-3: Lithostratigraphic profile and casing scheme for the STA2-1 borehole[4]

[4] For detailed information see Dossier I and III.

Tab. 1-2: Core and log depth for the main lithostratigraphic boundaries in the STA2-1 borehole[5]

System / Period	Group	Formation		Core depth in m (MD)	Log depth in m (MD)	
Quaternary				**26.0**		—
Paleogene + Neogene	OMM			62.0		—
	USM			422.0		—
	Siderolithic			**433.0**		—
Jurassic	Malm	«Felsenkalke» + «Massenkalk»		548.35	548.62	—
		Schwarzbach Formation		575.08	575.45	—
		Villigen Formation		646.23	646.63	—
		Wildegg Formation		727.18	728.20	—
	Dogger	Wutach Formation		732.16	733.25	—
		Variansmergel Formation		734.92	735.95	—
		«Parkinsoni-Württembergica-Schichten»		767.02	768.05	—
		«Herrenwis Unit»		777.54	778.47	—
		«Humphriesioolith Formation»		779.34	780.27	—
		Wedelsandstein Formation		786.85	787.79	—
		«Murchisonae-Oolith Formation»		799.67	800.67	—
		Opalinus Clay		905.20	906.87	—
	Lias	Staffelegg Formation		**940.89**	**941.42**	—
Triassic	Keuper	Klettgau Formation		969.87	970.52	—
		Bänkerjoch Formation		1043.07	1043.62	—
	Muschelkalk	Schinznach Formation		1116.01	1116.69	—
		Zeglingen Formation		1184.72	1185.42	—
		Kaiseraugst Formation		1224.20	1225.07	—
	Buntsandstein	Dinkelberg Formation		**1237.01**	**1237.94**	—
Permian	Rotliegend	Weitenau Formation	final depth	1288.12	1288.87	

[5] For details regarding lithostratigraphic boundaries see Dossier III and IV; for details about depth shifts (core goniometry) see Dossier V.

1.3 Documentation structure for the STA2-1 borehole

NAB 22-02 documents the majority of the investigations carried out in the STA2-1 borehole, including laboratory investigations on core material. The NAB comprises a series of stand-alone dossiers addressing individual topics and a final dossier with a summary composite plot (Tab. 1-3).

This documentation aims at early publication of the data collected in the STA2-1 borehole. It includes most of the data available approximately one year after completion of the borehole. Some analyses are still ongoing (e.g. diffusion experiments, analysis of veins, hydrochemical interpretation of water samples) and results will be published in separate reports.

The current borehole report will provide an important basis for the integration of datasets from different boreholes. The integration and interpretation of the results in the wider geological context will be documented later in separate geoscientific reports.

Tab. 1-3: List of dossiers included in NAB 22-02

Black indicates the dossier at hand.

Dossier	Title	Authors
I	TBO Stadel-2-1: Drilling	P. Hinterholzer-Reisegger
II	TBO Stadel-2-1: Core Photography	D. Kaehr & M. Gysi
III	TBO Stadel-2-1: Lithostratigraphy	P. Jordan, P. Schürch, H. Naef, M. Schwarz, R. Felber, T. Ibele & H.P. Weber
IV	TBO Stadel-2-1: Microfacies, Bio- and Chemostratigraphic Analyses	S. Wohlwend, H.R. Bläsi, S. Feist-Burkhardt, B. Hostettler, U. Menkveld-Gfeller, V. Dietze & G. Deplazes
V	TBO Stadel-2-1: Structural Geology	A. Ebert, S. Cioldi, E. Hägerstedt & H.P. Weber
VI	TBO Stadel-2-1: Wireline Logging, Micro-hydraulic Fracturing and Pressure-meter Testing	J. Gonus, E. Bailey, J. Desroches & R. Garrard
VII	TBO Stadel-2-1: Hydraulic Packer Testing	R. Schwarz, R. Beauheim, S.M.L. Hardie & A. Pechstein
VIII	TBO Stadel-2-1: Rock Properties, Porewater Characterisation and Natural Tracer Profiles	C. Zwahlen, L. Aschwanden, E. Gaucher, T. Gimmi, A. Jenni, M. Kiczka, U. Mäder, M. Mazurek, D. Roos, D. Rufer, H.N. Waber, P. Wersin & D. Traber
IX	TBO Stadel-2-1: Rock-mechanical and Geomechanical Laboratory Testing	E. Crisci, L. Laloui & S. Giger
X	TBO Stadel-2-1: Petrophysical Log Analysis	S. Marnat & J.K. Becker
	TBO Stadel-2-1: Summary Plot	Nagra

1.4 Scope and objectives of this dossier

The dossier at hand describes the results of the stochastic petrophysical log analysis performed in the STA2-1 borehole. The detailed workflow for this analysis is described in a methodology report (Marnat & Becker 2021, NAB 20-30). Here, only a very short summary is given. The lowest vertical resolution tools, such as ECS, Gamma Ray or Sonic, are limiting the resolution of the MultiMin analysis. High resolution and standard tools cannot be mixed in the same processing. For this reason, only the standard resolution version of the logs was input with a sampling rate of ½ foot (~ 15 cm).

For the Multimineral Log Analysis (abbreviation MultiMin throughout this report), a mineral content is assumed at each of these measurement locations, either from prior knowledge or from mineralogical lab analyses. A theoretical log response from this assumed mineral content for each available petrophysical log is calculated and compared to the measured log. Using optimisation techniques, the difference (i.e. the error) between calculated log responses and measured petrophysical logs is minimised by adjusting the assumed mineral content. Any deviation from this workflow is explained in this report.

The result of this analysis therefore are continuous profiles of the mineralogical content and other rock parameters (e.g. porosity) where the main aim of these calculations here were continuous profiles of the clay content and porosity.

The organisation of this dossier follows the necessary steps of the workflow. First, data is collected, and quality checks (QC) are performed. In addition, necessary pre-calculations concerning important environmental parameters are performed (Chapter 2). This is followed by the actual analysis of the data (Chapter 3) and a short description of results in Chapter 4. Chapter 4 also includes an estimation of the fit of the results to available data from lab measurements.

All depths in this report are reported as measured depths from top rig cellar (MD) if not stated otherwise.

2 Data preparation

2.1 Used log data

The acquisition, QC (quality control) and generation of log composites of the petrophysical logs from the borehole STA2-1 is described in more detail in Dossier VI, the raw corrected log data is also shown in Plate 1. Note that abbreviations in brackets in the list below are according to Schlumberger (SLB) mnemonics (as SLB was the log contractor responsible for the log acquisition). A detailed description of how the different tools measure the respective parameters and the underlying physics behind these measurements is not the focus of this report and can be found in Dossier VI, Chapter 3.1. The petrophysical logs used for this study are listed below:

- **Calliper log** (EMS/PPC – Environmental Measurement Sonde/Powered Positioning Calliper). The calliper log uses several coupled pairs of mechanical arms (2 pairs with PPC, 3 pairs with EMS) to continuously measure the borehole shape in different orientations.
- **Gamma Ray** (ECGR_EDTC, from the EDTC – Enhanced Digital Telemetry Cartridge). This log measures the naturally occurring radioactivity which can be used to determine the mineral content (mainly clay)
- **Spectral Gamma Ray** (SGR, from the HNGS – Hostile Natural Gamma Ray Sonde). This tool also measures the naturally occurring radioactivity. In addition to the total radioactivity, the tool is able to determine the amount (in ppm or wt.-%) of uranium (U), thorium (Th) and potassium (K) in the rocks which can be used e.g. for clay typing.
- **Neutron Hydrogen Index** (APLC curve, from APS – Accelerator Porosity Sonde). The APS is a tool that can measure the neutron hydrogen index in water saturated formations.

  This measurement is corrected for environmental effect and normalised to limestone matrix. SLB refers to this corrected curve as APLC (Near/Array Corrected Limestone Porosity). In addition, the APS can be used to determine **Sigma** (SIGF), a measure to determine the water content and mineralogical characterisations.
- **Density** (TLD – Three-detector Lithology Density). TLD is an induced radiation tool that measures the bulk density of the formation and the photoelectric factor (PEF). It uses a radioactive source to emit gamma photons into the formation. The gamma rays undergo Compton scattering by interacting with the atomic electrons in the formation. Compton scattering reduces the energy of the gamma rays in a stepwise manner and scatters the gamma rays in all directions. When the energy of the gamma rays is less than 0.5 MeV, they can undergo photoelectric absorption by interacting with the atomic electrons. The flux of gamma rays that reach each of the detectors of the TLD is therefore attenuated by the formation, and the amount of attenuation is dependent upon the electronic density of the formation, which is related to its bulk density. In addition, the TLD provides the **photoelectric absorption index** (photoelectric factor – PEF), which represents the probability that a gamma photon will be photo-electrically absorbed per electron of the atoms that compose the material. The PEF characterises the mineralogy. The TLD tool is housed in the High-Resolution Mechanical Sonde that also includes the Micro-Cylindrically Focused Log (MCFL) sonde, that measures the micro-resistivity or alternatively, the resistivity very close to the borehole wall (RXOZ).
- **Element Spectroscopy** (ECS – Elemental Capture Spectroscopy). The ECS is also an induced radiation tool with a radioactive neutron source. The ECS measures the concentration of a series of elements in the formation by analyzing the spectrum of back scattered gamma rays. The following elements are used in this report: DWSI_WALK2 (Si), DWCA_WALK2 (Ca), DWFE_WALK2 (Fe), DWSU_WALK2 (S), DWTI_WALK2 (Ti). Special processing techniques allow, under certain circumstances, the measurement of supplementary elements

such as Mg (MGWALK closure model, DWMG _MGWALK curve); Al, K and Na (ALKNA closure model, with ALKNA suffix), the two first being used in this study. The element spectroscopy measurements are provided in weight concentration (W/W).

During the QC process of the ECS acquisition, the DWMG_MGWALK response could be validated in the pure dolomites, reading close from the theoretical endpoint for dolomites: 0.132 W/W.

The iron concentration from the ECS WALK2 model was found systematically overestimating the XRF measurements on core samples. A correction was performed founded on the ECS and XRF results in MAR1-1. The resulting iron concentration curve was called DWFE_CORR.

The potassium content from ALKNA or MGWALK closure models were used where the HNGS could not be acquired due to longer tool offset.

The following correction was applied to DWK_ALKNA:

HFK_DWK_ALKNA = 1.87731 * DWK_ALKNA – 0.015928

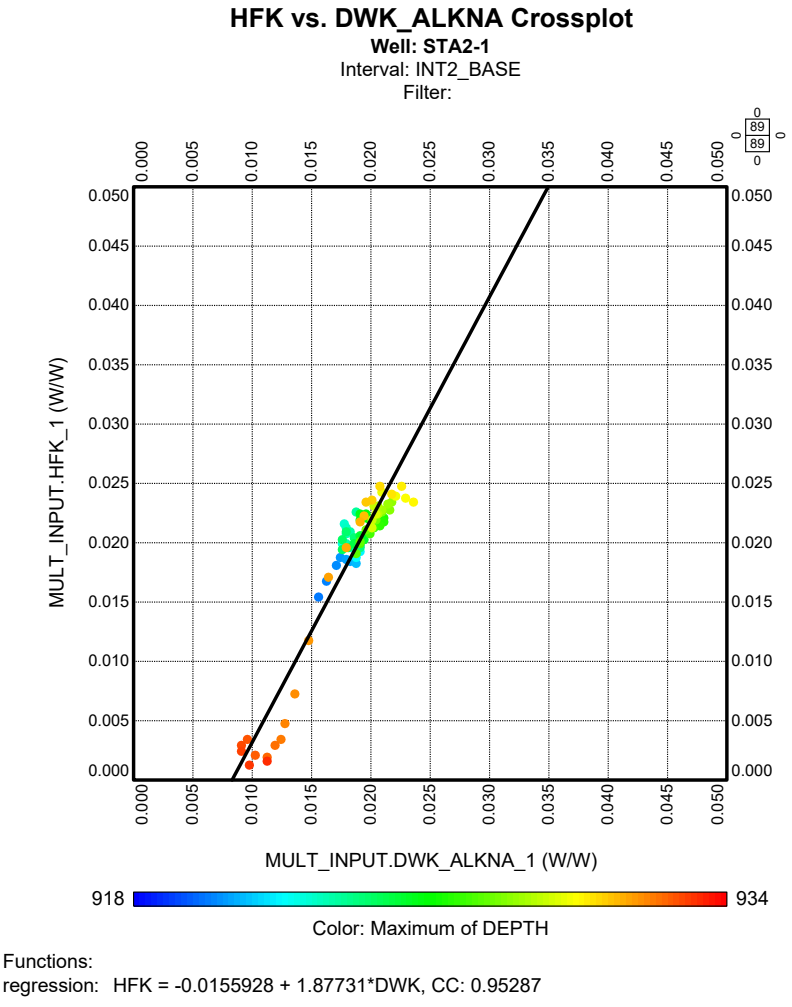

Fig. 2-1: HNGS HFK versus ECS DWK_ALKNA in INT2A

The following correction was applied to DWK_MGWALK:

HFK_DWK_MGWALK = 1.1973 * DWK_ALKNA – 0.00653712

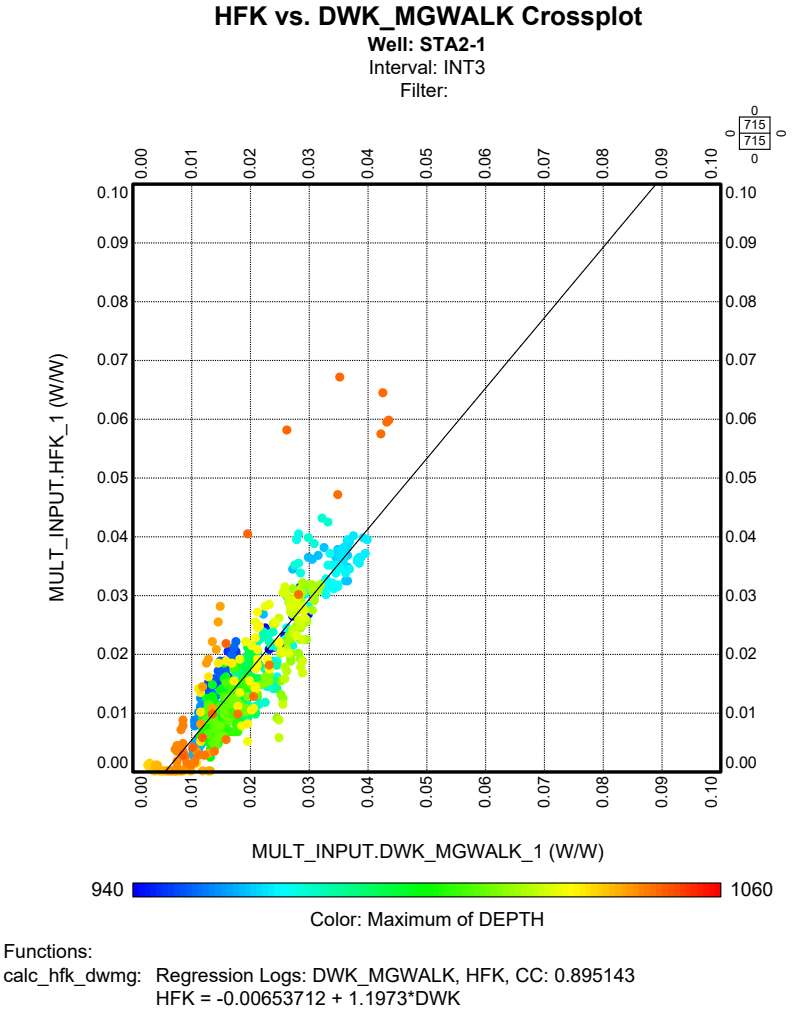

Fig. 2-2: HNGS HFK versus ECS DWK_ALKNA in INT3

The aluminium content from the ALKNA closure model was compared to the core XRF measurements. As the measurements are close (Fig. 2-4), DWAL_ALKNA was used as an input curve for the MultiMin models.

- **Resistivity** (HRLT – High Resolution Laterolog array Tool). The HRLT measures the formation electrical resistivities at different depths of investigation, providing a mud filtrate invasion profile, if any invasion. Processing allows the extrapolation of the resistivity measurements far into the formation (true formation resistivity), as well as close to the borehole wall (micro-resistivity). The resistivity is a function of the water content of the formation and its salinity.
- **Sonic** (MSIP – Modular Sonic Imaging Platform. The MSIP measures the formation interval transit time, a measure of how fast seismic waves (compressional, shear and Stoneley waves) propagate through the formation.

An overview of the used petrophysical logs and their measurements in the STA2-1 borehole is given in Plate 1.

Usable log data were available for analysis from 470.5 to 1'284.0 m (see Plate 1). Due to gaps between drilling sections and cased hole sections (see Dossier I), two minor MultiMin interpretation gaps, due to insufficient petrophysical log coverage, remained in the following intervals, as shown in Fig. 2-3:

- 934.4 – 936.3 m (between Runs 2.1.X and Runs 3.1.X)
- 1049.5 – 1051.2 m (between Runs 3.1.X and Runs 4.1.X)

In the upper interval (0 – 470.5 m driller's depth), only technical logging was performed (Dossier VI) which is not suitable for the log interpretation routines used here (only caliper, gamma ray and cement evaluation are available. However, this interval is only of minor interest in terms of formation characterisation for the geological disposal of radioactive waste and, hence, was disregarded completely.

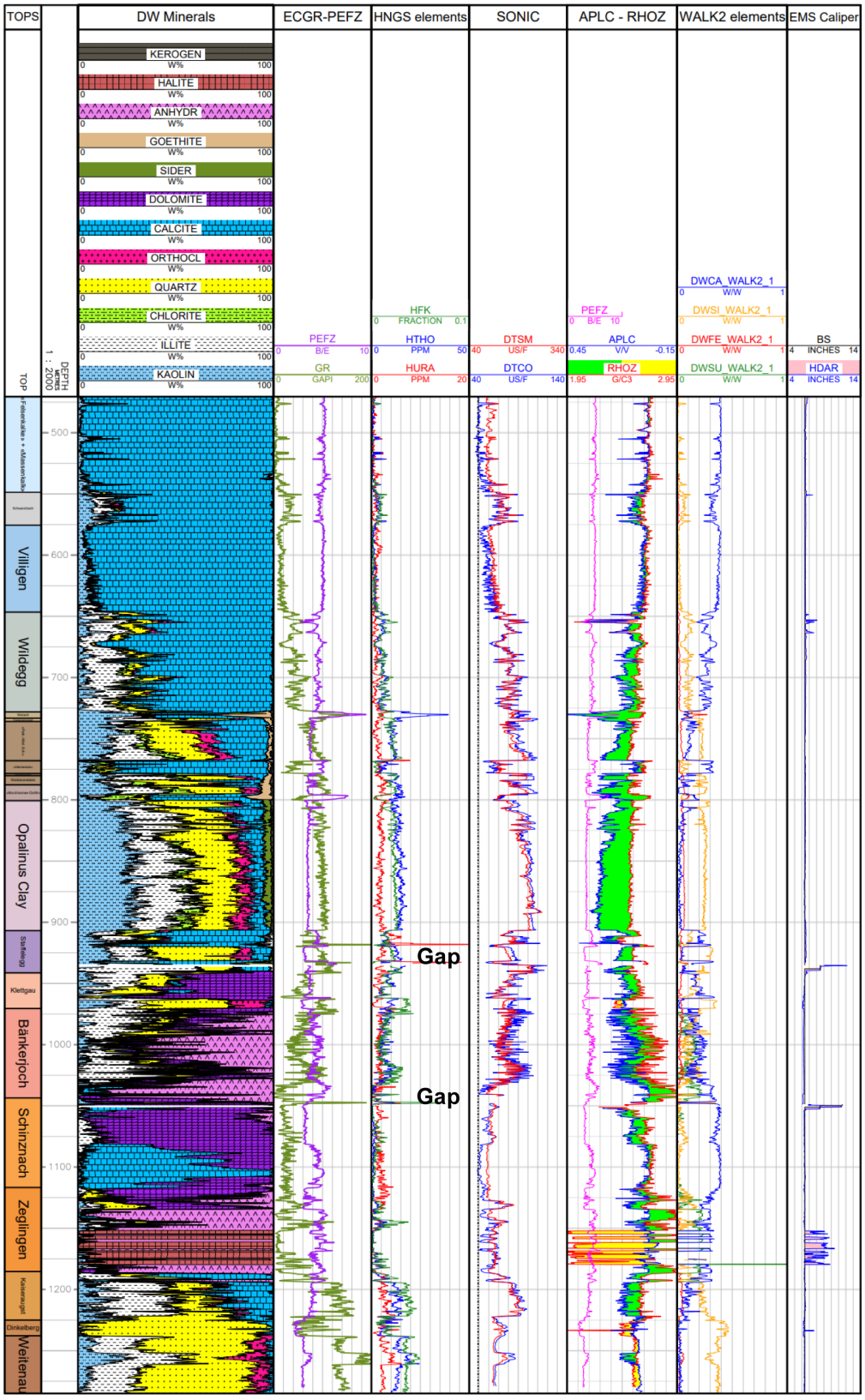

Fig. 2-3: Petrophysical log availability and short gaps in the STA2-1 borehole

Please note that ECS elements are displayed as measured (in weight/weight, 0 – 1 w/w range) and are not converted to wt.-% (weight percentage) here.

2.2 Used core data

As previously mentioned, the MultiMin algorithm requires an initial assumption of the mineralogical content. For the calibration of the log interpretation, core data (lab measurements of mineralogy, total porosity and density) were used (see Dossier VIII for more details on core data, some core data is shown in Plates 1 and 2). 142 core samples collected at depth ranging from 476.47 to 1'177.49 m were available of which 98 were analysed for pycnometer total porosity and water loss total porosity, 92 for grain density, 79 for XRD mineralogy and 27 for clay types. The analysed minerals were quartz, K-feldspars, plagioclase, calcite, dolomite/ankerite, siderite, magnesite, barite, goethite, haematite, maghemite, magnetite, anhydrite, celestite, fluorite, pyrite, marcasite, clay minerals and organic carbon. The 27 samples analysed for clay typing (in the interval 633.23 – 963.35 m) quantified the illite, smectite, kaolinite and chlorite endmembers. The mineral content was used to calibrate the MultiMin interpretation.

As mentioned earlier, porosities and grain densities are also included in the core data and hence used for this study. The three measured porosities (water-loss porosity (105 °C) using bulk wet density, water-loss porosity (105 °C) using grain density and pycnometer porosity) were accounted for, the most relevant was selected compared to the MultiMin total porosity (PHIT Φ_t). The relative errors of these measurements are provided as well. For more details on the exact measurement procedures of these parameters see Waber (2020).

The difference between core and log depth were taken from the formation tops table (Dossier V) where the depths are available in driller and logger references. The amplitude of the shift was linearly interpolated between the formation tops, leading to some uncertainty in the core to log depth matching.

Part of the core data is also shown in Plate 2.

2.3 Multi-sensor Core Logger (MSCL) data

MSCL measurements from cores were available in the STA2-1 borehole (from 720.4 to 934.85 m), with a sampling rate of 0.05 m. Measurements were performed in the interval of the host rock (Opalinus Clay) and its confining units. The following parameters were measured:

- Bulk density in g/cc
- Compressional (P) wave velocity in m/s
- Spectral gamma ray curves: potassium (K, %), thorium (Th, ppm) and uranium (U, ppm)
- XRF (X-ray fluorescence) elemental analysis: iron (Fe), silicon (Si), calcium (Ca), aluminium (Al), titanium (Ti) and sulphur (S) are used for this study.

Some ECS data could not be acquired between drilling sections, leaving a gap. In this same interval, no XRF data is available to fill the gaps.

The XRF elemental analysis results were compared with the same elements concentration from the ECS logging (WALK2 closure model). The MSCL data (also referred to as core logs in this report) covers the measured interval at variable sampling rates (usually 0.05 m).

This comparison is shown in Fig. 2-4 for STA2-1, the core logs were not depth-shifted.

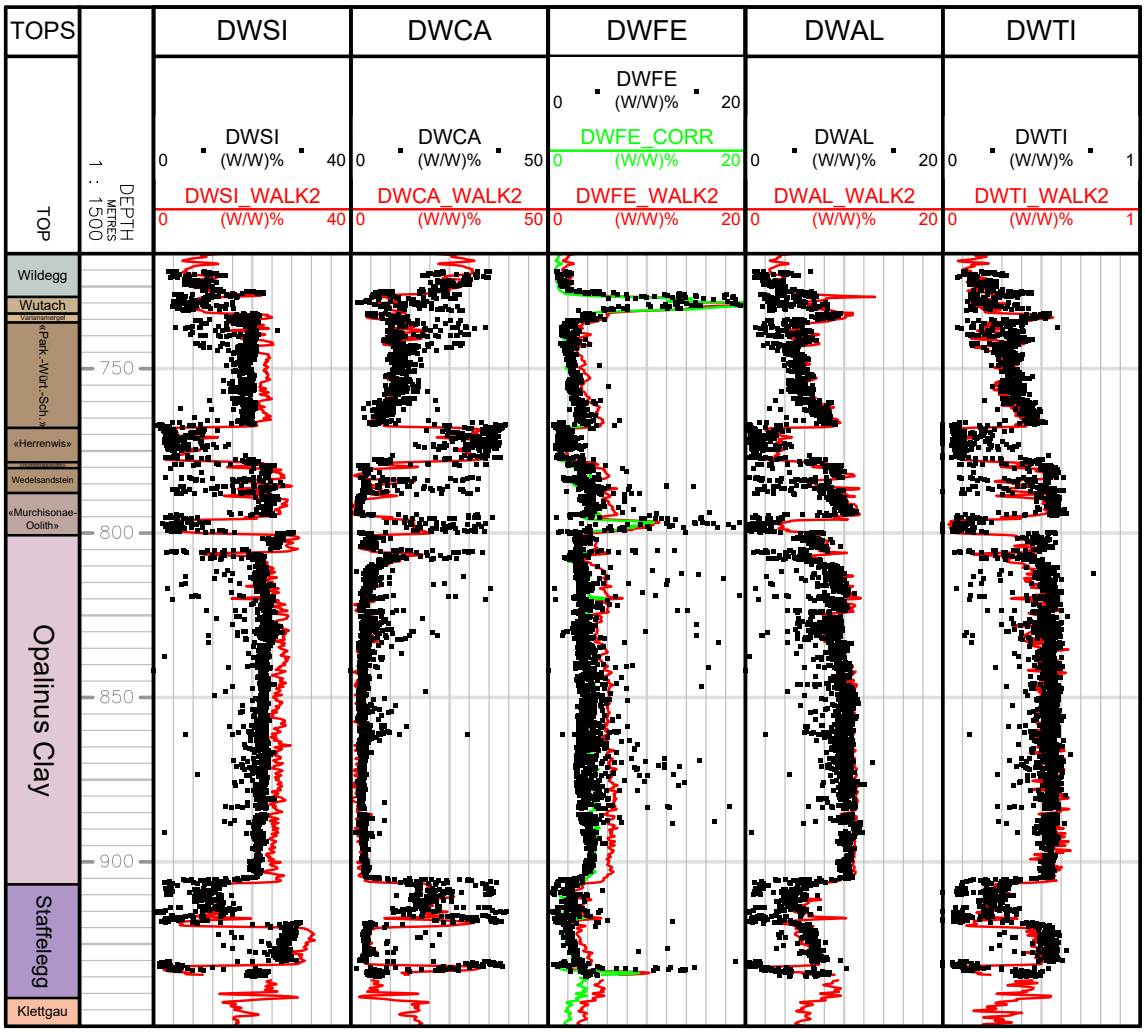

Fig. 2-4: XRF (black dots) and ECS WALK2 (red curves) elements comparison for STA2-1

While the calcium, aluminium (from the ALKNA closure model) and titanium concentrations are almost similar, the XRF iron and silicon are significantly lower than from the ECS WALK2 closure model.

The same bias on the iron content was already noticed in the recent MAR1-1 borehole, a correction was used based on the correlation between XRF iron and ECS DWFE_WALK2, using the following equation:

$$DWFE\_CORR = 0.0375 + 0.396 * DWFE\_WALK2 + 4.882 * DWFE\_WALK2^2$$

DWFE_CORR is displayed as a green curve in the iron track of Fig. 2-4.

The same check was done for the core and HNGS spectral gamma ray (see Fig. 2-5) in STA2-1.

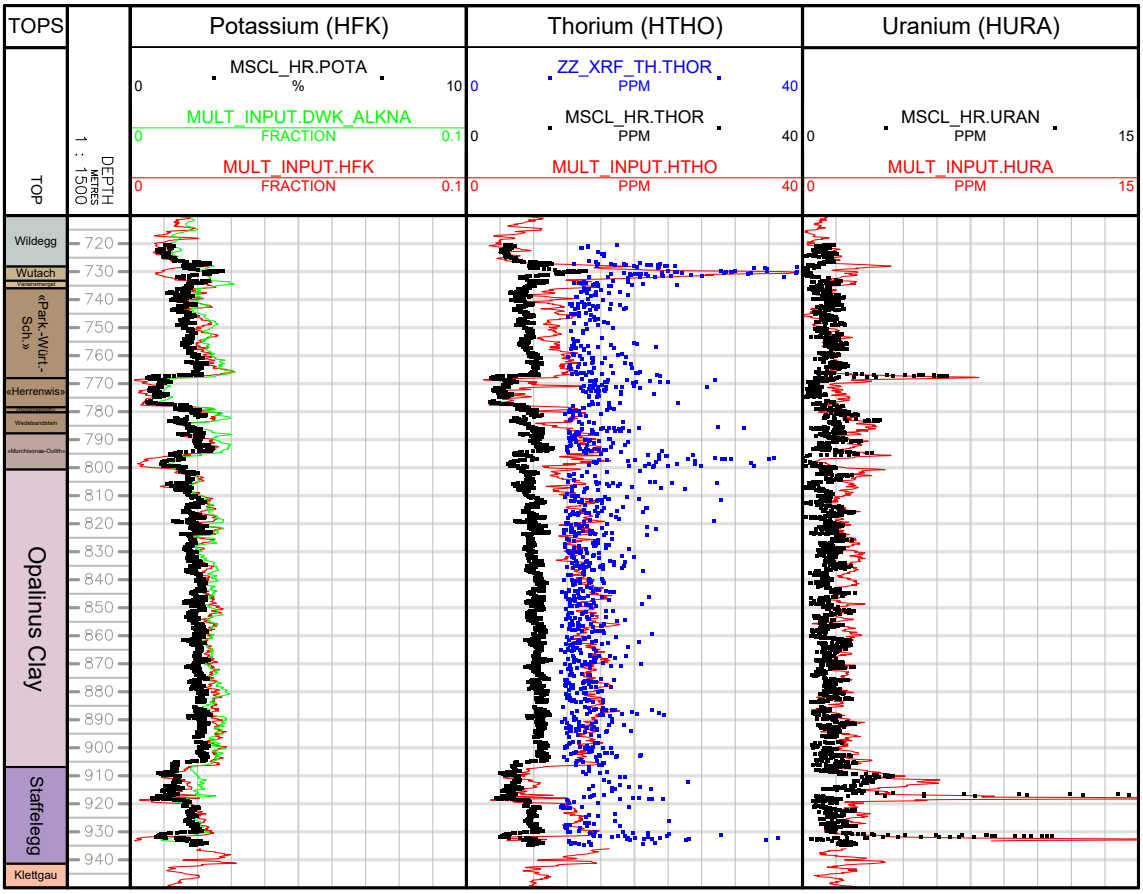

Fig. 2-5: Core (black dots: spectral gamma ray, blue dots XRF thorium) and wireline HNGS (red curves) spectral gamma ray elements comparison

The potassium from MSCL is slightly lower than the HFK from HNGS and the DWK_ALKNA. The MSCL uranium is close but locally inconsistent with HURA.

The HTHO from HNGS is often much higher than the thorium content measured with the MSCL. The XRF thorium (blue dots) is not usable, showing too much dispersion; it is roughly in line with the HTHO curve.

Hence, the MSCL data was used indirectly for a QC and subsequently to correct petrophysical log measurements, namely the iron content of the ECS measurements.

2.4 MultiMin input dataset preparation

The petrophysical composite log used as input for this study (see Dossier VI) represents a quality controlled, edited, corrected and merged dataset for a selection of the most important petrophysical logging data recorded in each section of the borehole. As mentioned earlier, two gaps in the coverage of the borehole with petrophysical logs occur. The original measurements and corrections of the petrophysical logs are reported in Dossier VI.

The only deviation to this source dataset is the use of the corrected DWFE_CORR.

2.5 Preliminary calculations (Precalc)

As the wireline logs measure parameters under in situ conditions (e.g. temperatures depending on depth and temperature of the borehole fluid, infiltration of mud into the formation depending on the borehole fluid and its density etc.), these prevailing conditions in the borehole have to be taken into account to correctly predict/calculate the theoretical log response from the assumed mineral and fluid content (i.e. total porosity) at a certain depth. Continuous profiles of these environmental parameters were calculated using the Precalc module from the interpretation software Geolog. The main parameters used for the calculation of these environmental parameters are, for reasons of transparency and to be able to replicate exactly the analyses reported here, displayed in Appendix A.

The mud properties (mud density and resistivities) reported here were extracted from the validated SLB wireline log headers (see Dossier VI).

3 Petrophysical log interpretation

3.1 MultiMin interpretation

In the following, the petrophysical log interpretation and its results are shortly described. All necessary data treatment and environmental pre-calculations have been described in the previous chapters or are described in the Methodology report (Marnat & Becker 2021). Many qualitatively good wireline logs were available in most of the borehole, allowing the computation of many unknowns (fluids and minerals).

Significant hydrocarbon shows were neither described by the mudlogging nor inferred from cores or petrophysical logs. Consequently, the formations were treated as water wet (i.e. with saline water as the pore fluid).

The main minerals were inferred from the XRD measurements on STA2-1 and previous boreholes core samples (Dossiers VIII of the respective borehole reports), Weiach-1 and Benken-1 from Mazurek (2017). Using the MultiMin approach, the mineral content for the following minerals were modelled:

- Clay mineral endmembers (kaolinite, illite, smectite and chlorites) and total clay mineral content. From the available wireline logs, the smectite cannot be differentiated from the kaolinite
- Silicates: quartz and plagioclases, potassic feldspars
- Carbonates: calcite, siderite (also an iron-rich mineral), dolomite/ankerite
- Iron-rich minerals: siderite, pyrite and goethite, consistently with the iron content measured by both the ECS tool and the XRF on core samples
- Evaporites: anhydrite and halite
- Organic carbon (kerogen)

These compounds were modelled depending on the available data. In case not enough data were available for a given interval (e.g. where data was missing or of insufficient quality), some minerals were merged to a pseudo-mineral to reduce the number of unknowns (see Marnat & Becker 2021 for more details).

Tab. 3-1 shows an example of the interpretation intervals, the available data and the MultiMin model names used in each interval. The intervals are defined based on their consistent mineralogy, available logs and consistent environmental parameters (e.g. mud system changes). Interpretation intervals may be subdivided further, e.g. to respect a reduced data quality. The full table with all intervals is available in Appendix B.

Mineral and fluid endpoints were manually optimised to both reduce the difference between measured and predicted logs and match the core mineralogy and porosity. Greatly simplified, an endpoint can be regarded as a factor that is used to calculate the theoretical log response for each mineral (e.g. if it is assumed that the endpoint for the density of calcite is 2.71 g/cc, a mineral content of 100% calcite should result in a density of 2.71 g/cc of the predicted density log). For a detailed explanation see Marnat & Becker (2021).

Tab. 3-1: List of MultiMin models used in STA2-1

The intervals (column Interval name) may include several MultiMin models if some of the input data were of bad quality or the particular section of the interval required special assumptions due to its assumed mineralogy.

The column Cond Num stands for model condition number. Low values are typical for good mathematical models (below 4.00). Condition numbers above 4.00 highlighted in yellow correspond to fair models, while values above 5.00 correspond to bad models. See Section 3.2 for more information.

From (m)	To (m)	Interval name	Multimin Models	Cond Num	Description
470.5	550.0	INT1	sta21_int1	3.56	Malm
550.0	551.0	INT1	sta21_int1_bh	3.45	HDRA peak
551.0	640.0	INT1	sta21_int1	3.56	Malm
640.0	648.0	INT2_TOP	sta21_int2_top	3.95	Wildegg
648.0	649.0	INT2_TOP	sta21_int2_top_bh	4.19	Wildegg
649.0	652.3	INT2_TOP	sta21_int2_top	3.95	Wildegg
652.3	653.4	INT2_TOP	sta21_int2_top_bh	4.19	Wildegg
653.4	653.8	INT2_TOP	sta21_int2_top	3.95	Wildegg
653.8	655.9	INT2_TOP	sta21_int2_top_bh	4.19	Wildegg
655.9	662.0	INT2_TOP	sta21_int2_top	3.95	Wildegg
662.0	663.7	INT2_TOP	sta21_int2_top_bh	4.19	Wildegg
663.7	727.7	INT2_TOP	sta21_int2_top	3.95	Wildegg
727.7	733.0	INT2_TOP	sta21_int2_wut	2.78	Iron-rich Wutach Formation
733.0	778.0	INT2_TOP	sta21_int2_top	3.95	Brauner Dogger
778.0	799.7	INT2_TOP	sta21_int2_sid	3.96	Brauner Dogger, siderite
799.7	919.8	INT2	sta21_int2	4.18	Opalinus Clay & Staffelegg
919.8	926.0	INT2_BASE	sta21_int2_base	3.85	Staffelegg
926.0	932.0	INT2_BASE	sta21_int2_base_noct	3.85	Staffelegg, no Ct
932.0	933.3	INT2_BASE	sta21_int2_base_noaps	5.58	Staffelegg, no APS
933.3	934.4	INT2_BASE	sta21_int2_base_nohngs	6.93	Staffelegg, no APS, no HNGS
934.4	935.7		No model		Not enough logs
935.7	936.3	INT2_BASE	sta21_int2_base_noct	3.85	Staffelegg, no Ct
936.3	940.0	INT2_BASE	sta21_int2_base	3.85	Staffelegg
940.0	963.0	INT3	sta21_int3	2.98	Klettgau-Bänkerjoch
963.0	970.0	INT3	sta21_int3_sd	2.52	Sandy bed
970.0	997.2	INT3	sta21_int3	2.98	
997.2	997.8	INT3	sta21_int3_nodt	2.84	Bänkerjoch, no Sonic
997.8	1015.9	INT3	sta21_int3	2.98	Bänkerjoch
1015.9	1016.1	INT3	sta21_int3_nodt	2.84	Bänkerjoch, no Sonic
1016.1	1041.1	INT3	sta21_int3	2.98	Bänkerjoch
1041.1	1047.3	INT3	sta21_int3_nodt	2.84	Bänkerjoch-Schinznach, no DT
1047.3	1048.0	INT3	sta21_int3_nodt_noaps	2.44	Schinznach, no Sonic, no APS
1048.0	1048.9	INT3	sta21_int3_noaps	2.44	Schinznach, no APS
1048.9	1049.5	INT3	sta21_int3_noaps_nohngs	2.44	Schinznach, no APS, no HNGS

Tab. 3-1: (continued)

From (m)	To (m)	Interval name	Multimin Models	Cond Num	Description
1049.5	1051.2		No model		Not enough logs
1051.2	1051.8	INT4	sta21_int4_noaps	3.50	Schinznach, no APS
1051.8	1052.6	INT4	sta21_int4_bad_dn	3.45	Schinznach, badhole
1052.6	1123.0	INT4	sta21_int4	3.91	Schinznach, Zeglingen
1123.0	1124.7	INT4_Base	sta21_int4_base	3.92	Zeglingen
1124.7	1126.4	INT4_Base	sta21_int4_base_nodt	3.92	Zeglingen, no Sonic
1126.4	1151.8	INT4_Base	sta21_int4_base	2.69	Zeglingen
1151.8	1155.1	INT4_SALT	sta21_int4_salt	1.57	Halite layer
1155.1	1156.1	INT4_SALT	sta21_int4S	2.69	Zeglingen
1156.1	1159.1	INT4_SALT	sta21_int4_salt	1.57	Halite layer
1159.1	1161.2	INT4_SALT	sta21_int4S	2.69	Zeglingen
1161.2	1166.9	INT4_SALT	sta21_int4_salt	1.57	Halite layer
1166.9	1168.2	INT4_SALT	sta21_int4S	2.69	Zeglingen
1168.2	1175.1	INT4_SALT	sta21_int4_salt	1.57	Halite layer
1175.1	1175.0	INT4_SALT	sta21_int4S	2.69	Zeglingen
1176.0	1179.8	INT4_SALT	sta21_int4_salt	1.57	Halite layer
1179.8	1187.1	INT4_SALT	sta21_int4S	2.69	Zeglingen
1187.1	1217.5	INT5	sta21_int5	4.03	Kaiseraugst
1217.5	1218.9	INT5	sta21_int5_nodt	4.03	Kaiseraugst, no Sonic
1218.9	1224.9	INT5	sta21_int5	4.03	Kaiseraugst
1224.9	1231.8	INT6	sta21_int6	3.21	Dinkelberg
1231.8	1233.1	INT6	sta21_int6_nodt	4.59	Dinkelberg, no Sonic
1233.1	1233.8	INT6	sta21_int6_bh	3.48	Dinkelberg, badhole
1233.8	1238.1	INT6	sta21_int6	3.21	Dinkelberg
1238.1	1277.7	INT7	sta21_int7	3.47	Weitenau
1277.7	1279.6	INT7	sta21_int7_noct	3.47	Weitenau, no Ct
1279.6	1284.8	INT7	sta21_int7_notld	4.45	Weitenau, no density/Pef

Based on expert judgement, an uncertainty value for the petrophysical logs was estimated and used to adjust the weight given to the respective log in the MultiMin computation. Again, greatly simplified, if the uncertainty values are large, the corresponding log response will be predicted in the MultiMin interpretation, but it will not be used in the process of error minimisation and hence has no impact on the result of the MultiMin interpretation (for more details see Marnat & Becker 2021). High uncertainty values often apply to the Sonic curves, the PEFZ (as PEFZ is already used for the U computation, Photo-electric cross-section) and the electrical conductivities.

The detailed parameters for all the MultiMin models are available in tables in Appendix C.

3.2 Bad hole treatment and quality of results

The quality of the MultiMin interpretation relies in part on the quality of the input data. However, it also relies on the number of available curves and the number of unknowns (i.e. minerals) that need to be calculated. Hence, several quality indicators exist that either are informative about the quality of the input data (LQC-Index), the definition of the mathematical model (CONDNUM, NFUN) or the quality of the interpretation results (MULT_QC and QUALITY).

3.2.1 Indicator for input data quality (LQC_INDEX)

During each wireline logging, the borehole shape is determined using a calliper log. If the borehole shape deteriorates far from the bit size (BS) and bit shape (usually circular), some (or all) of the wireline logs may measure biased data because the distance between the tool and the borehole wall is too large. In that case, the response of a considerable amount of borehole fluid is measured by the tool and the measurements represent more the petrophysical parameters of the borehole fluid than of the formation.

Four bad hole indicators, which can be used as a quality measure of the data, are calculated from some of the available wireline logs:

1. FLAG_UNFIT_ND: Neutron-Density crossplot, flagging bad hole and unusual mineralogical settings from expert picking in the density-neutron crossplot
2. FLAG_BADHOLE_OVERGAUGE: HDAR > 1.15 * Bit Size
3. FLAG_BADHOLE_RUGO: Borehole wall rugosity, HDRA > 0.025 g/cc: HDRA (bulk density correction) is a correction of the bulk density measured with a gamma-gamma type logging device (here TLD). If this correction factor is larger than 0.025 g/cc, the indicator is triggered
4. FLAG_BADHOLE_STOF: APS Neutron standoff > 0.35 in

For detailed information about these four indicators, please refer to Dossier VI.

These four indicators have two possible values: 0 in good hole or 1 in bad hole. They were combined to generate a log quality control flag (LQC_INDEX) using the following equation:

LQC_INDEX = (FLAG_BADHOLE_DN + FLAG_BADHOLE_OVERGAUGE +

FLAG_BADHOLE_RUGO + FLAG_BADHOLE_STOF) / 4

Hence, the value of the LQC-Index must be between 0 and 1 (and can only have values of 0, 0.25, 0.5, 0.75 or 1).

3.2.2 Indicator for the mathematical model (CONDNUM and NFUN)

CONDNUM

The CONDNUM stands for model condition number. Low values are typical for good mathematical models (below 4.00). Condition numbers above 4.00 correspond to fair models. A list of CONDNUMs for the different MultiMin interpretation intervals is given in Tab. 3-1. Please note that CONDNUM is not a proxy for the quality of the calculated output but only for the definition of the mathematical model to calculate the said output.

NFUN

NFUN indicates how many iterations were required to fulfil the constraints imposed by the available data where fewer numbers of iterations are indicative for a more robust model. NFUN is also shown in Plate 1. Please note that NFUN, as CONDNUM, is not a proxy for the quality of the calculated output but only for the definition of the mathematical model to calculate the said output.

3.2.3 Indicator for the MultiMin interpretation results (MULT_QC and QUALITY)

MULT_QC

The MultiMin results were not edited in STA2-1 (e.g. less reliable data were not removed from the interpretation results), but an integrative MultiMin QC flag was generated (MULT_QC) combining several of the aforementioned quality indicators to inform the data user of potentially invalid results. As this flag relies on the availability of lab measurements, it is only available where a respective lab measurement is available. The MULT_QC flag relies on expert judgement and can have values of 2, 1 or 0 based on the three different scenarios detailed below:

- Highly suspicious porosity spikes occur and usually are correlated to an LQC-Index above or equal to 0.5, the quality curve (displayed in Plates 1 and 2, see below) can show values above 2 and the MultiMin results do not match the core measurements: MULT_QC = 2. A value of 2 in MULT_QC corresponds to most likely unreliable data.
- Suspicious porosity spikes occur but with a usually acceptable LQC_Index (0 or 0.25) and MultiMin quality curve values below 2: MULT_QC = 1. This value indicates that results can/should be used for the characterisation of the formation but should be treated with caution as the interpreted results are not a perfect fit with the available data.
- Otherwise, MULT_QC = 0. Interpreted results are reliable and can be used to characterise the formation.

QUALITY

In addition, a quality curve is shown in Plates 1 and 2. This curve is an indication of how well the observed measurements from wireline logs and the predicted results are part of the same population. At a value of QUALITY less than one, the calculated accuracy is within 95% compared to the original wireline logs and therefore the analysis is of good quality. If the value is consistently above one, log measurements are not well honoured by the predicted curves, hence the analysis must be regarded as less robust.

Please note that the quality curve only compares the results of the MultiMin interpretation with the petrophysical logs and does not take data quality of the petrophysical logs (e.g. in bad hole sections) or lab measurements into account. The only indicator combining information on input data quality and interpretation result is the MULT_QC indictor detailed above.

4 Results of the calibrated stochastic log interpretation

In the following, the main results of the stochastic log interpretation are summarised. Plate 1 shows the measured wireline logs together with the calculated output from the MultiMin approach. The main results in terms of mineral content and porosity are displayed in Plate 2 as continuous curves. Plate 2 also shows the available lab measurements (from core data).

The aim of this chapter is not a detailed description and characterisation of the sedimentary sequence based on log interpretation results, but rather gives a more general description of the data and a general characterisation of the stratigraphic system or groups shown in Plate 2. Section 4.1 compares the interpretation results with core data giving an overview on the robustness of the interpreted mineralogical content in the borehole. Section 4.2 gives a general characterisation while Section 4.3 gives a more detailed description of calculated parameters in the Opalinus Clay.

4.1 Comparison of interpretation results with core data

Below, the MultiMin interpretations are compared to the mineralogical (bulk) and petrophysical measurements (porosity).

Due to the log database constraints and the need for robust mathematical MultiMin models (i.e. condition numbers ideally below 5 for fair to good models), the number of modelled minerals had to be adjusted. For the sake of easy comparison, the minerals had to be grouped:

- Quartz and feldspars (plagioclase and orthoclase) are grouped into a single pseudo-mineral (called QF-SILICATES in Plate 2).
- Different clay minerals were computed when possible (kaolinite – smectite together, chlorites: non-potassic clays, called NO_K_CLAYS, and illite). All clay minerals were added to a (total) clay content (DRY_CLAY).
- Comparable to the clay minerals, different carbonate minerals were also calculated (calcite, dolomite and siderite). In Plate 2, a track displays the total amount of carbonates (called CARBONATES). Next to it, two tracks show the calcite and dolomite content, as the latter two can be used to distinguish between some formations, especially below the Opalinus Clay.

Figs. 4-1 to 4-6 show crossplots between mineral weight percentages from cores (x-axis, from XRD lab analyses) and interpretation results from MultiMin (y-axis).

Fig. 4-7 shows the crossplot between total porosity from core (x-axis, Water-loss porosity (105 °C) using grain density lab measurement) and interpretation results from MultiMin (y-axis).

All available data are displayed together, covering the interval from the Villigen to the Schinznach Formations. The color coding represents the formations, as per the attached legend.

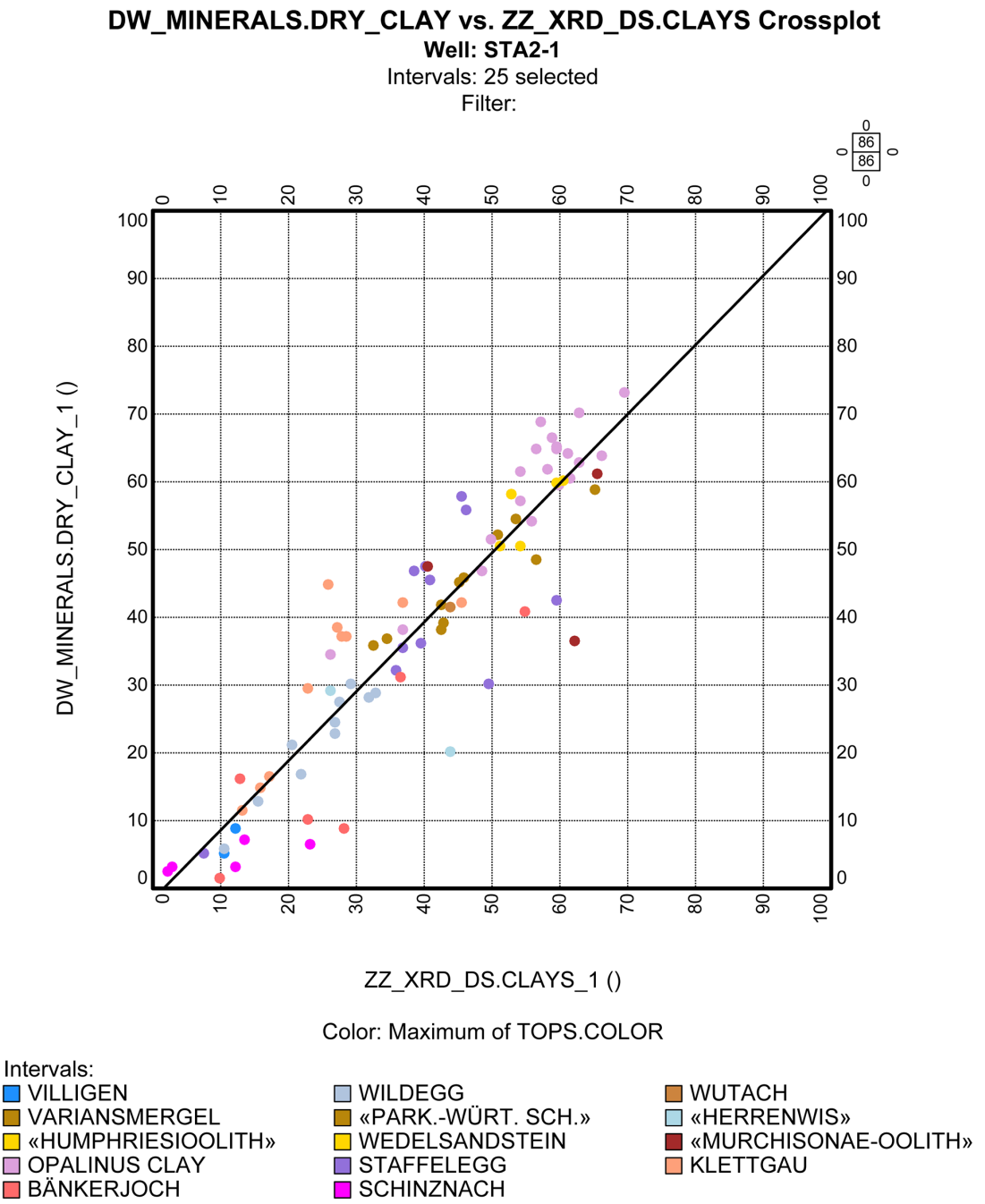

Fig. 4-1: Weight-% of dry clay (y-axis) compared to core XRD data (x-axis), Villigen to Schinznach Formation)

The MultiMin dry clay content is well correlated to the core XRD data (cc = 0.92).

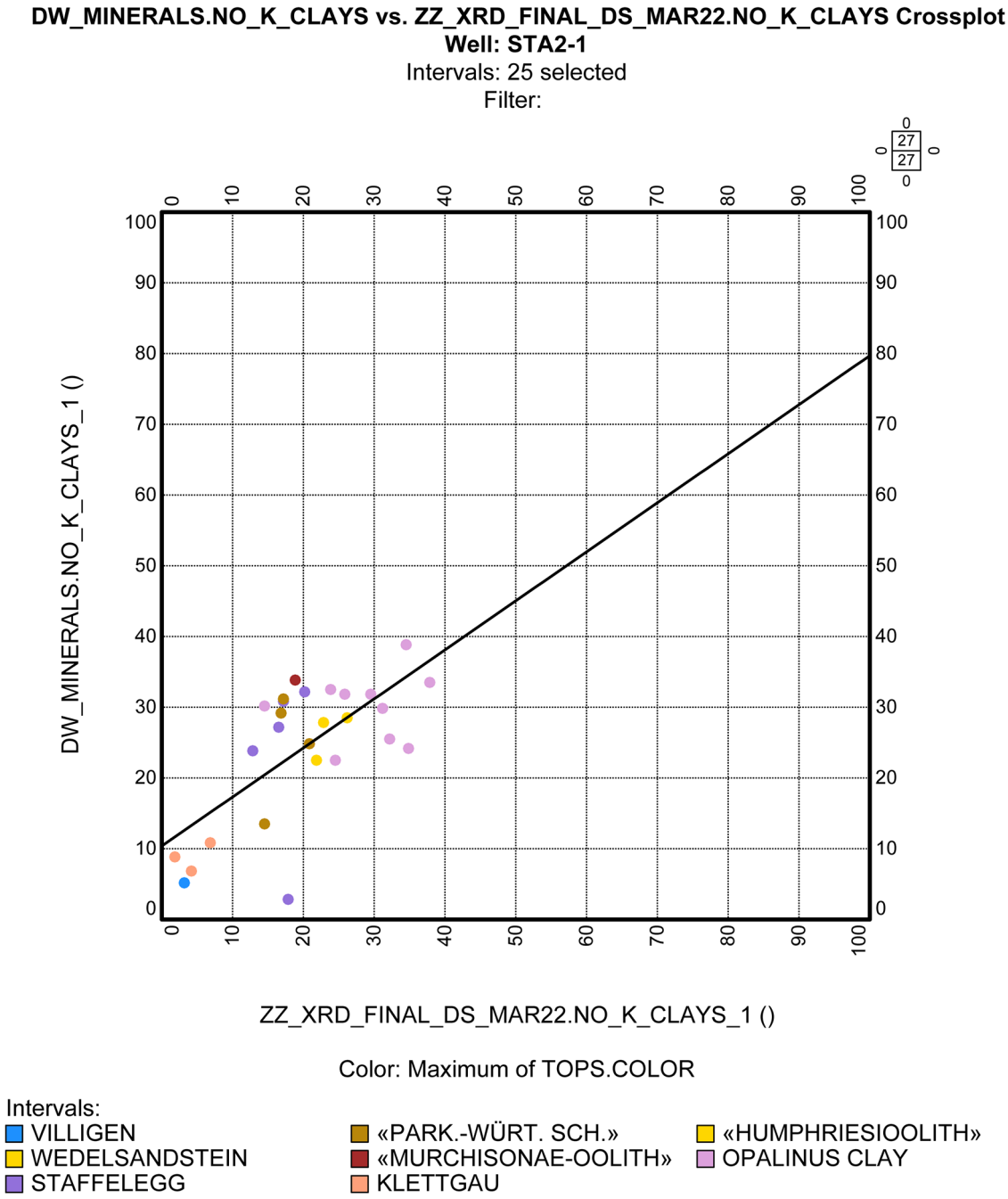

Fig. 4-2: Weight-% of non-potassic dry clay (y-axis) compared to core XRD data (x-axis), Villigen to Klettgau Formation

The XRD clay endmembers were not measured in all formations.

The MultiMin non-potassic clay content is fairly correlated to the core XRD data in the Opalinus Clay (light purple dots) but the dispersion remains large (overall cc = 0.68).

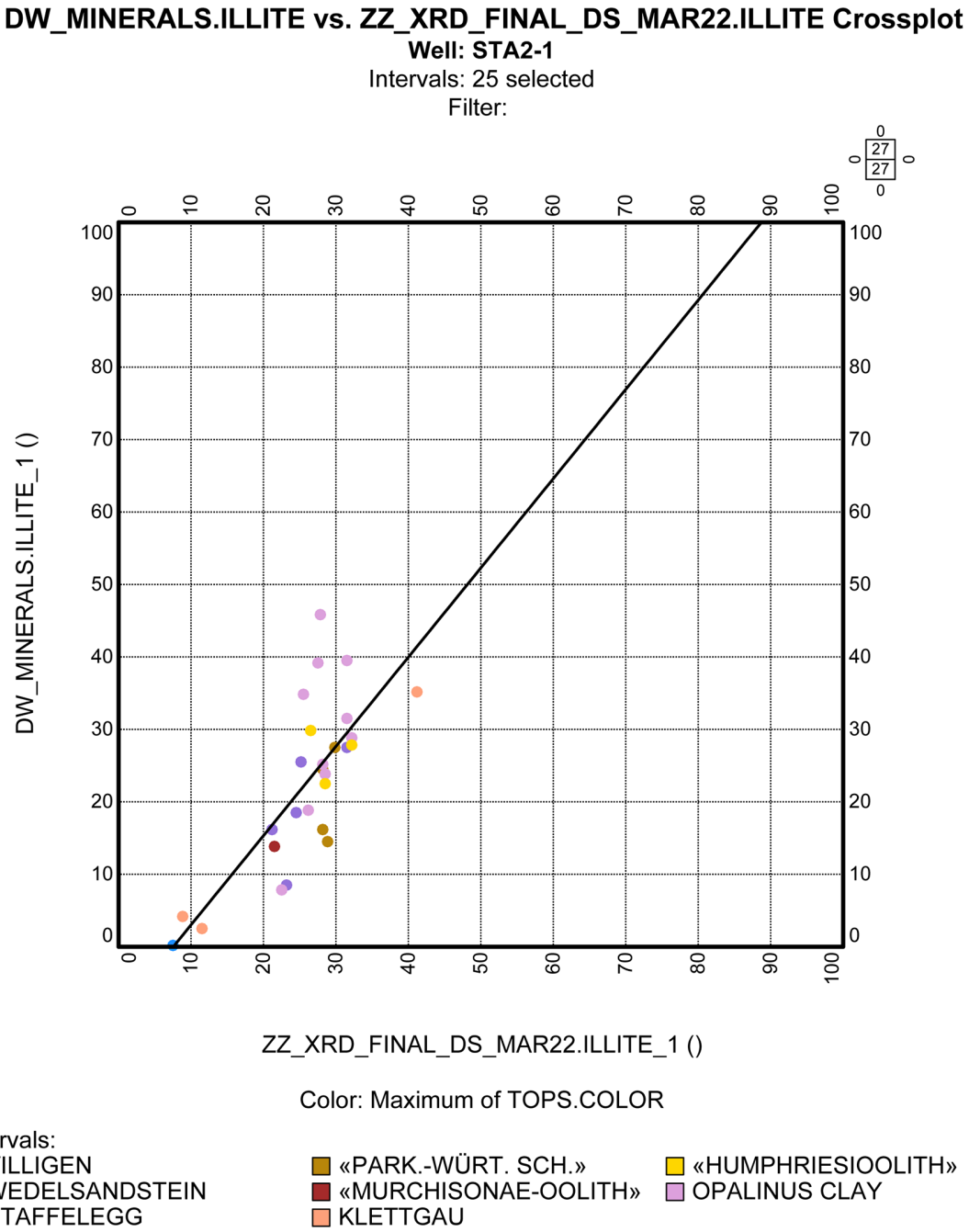

Fig. 4-3: Weight-% of illite (y-axis) compared to core XRD data (x-axis), Villigen to Klettgau Formation

The XRD clay endmembers were not measured in all formations.

The MultiMin illite content is not well correlated to the core XRD data (cc = 0.76).

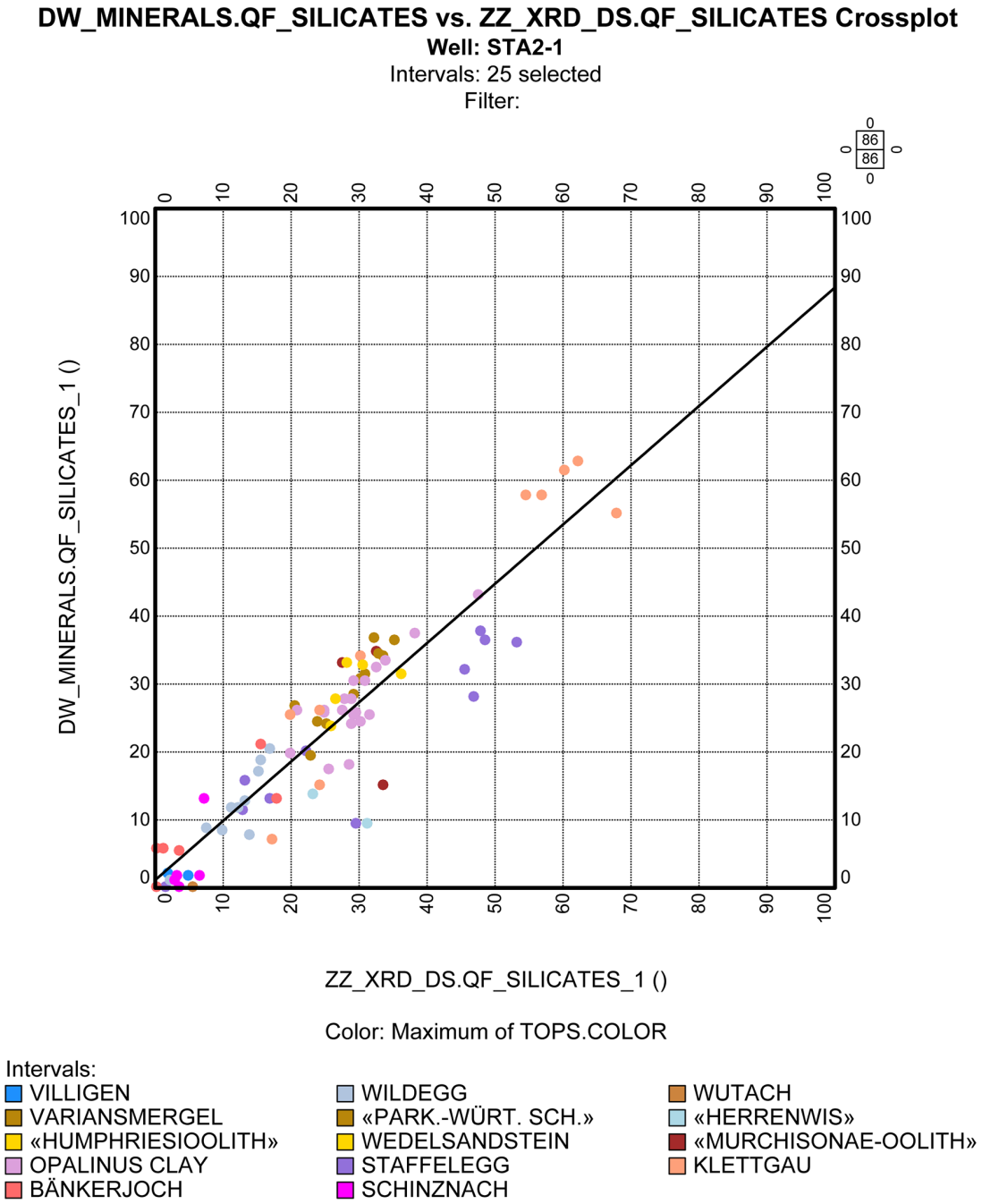

Fig. 4-4: Weight-% of QF-silicates (y-axis) compared to core XRD data (x-axis), Villigen to Schinznach Formation

The QF-silicates are the sum of quartz and feldspars. The calibration to core XRD data is good (cc = 0.91).

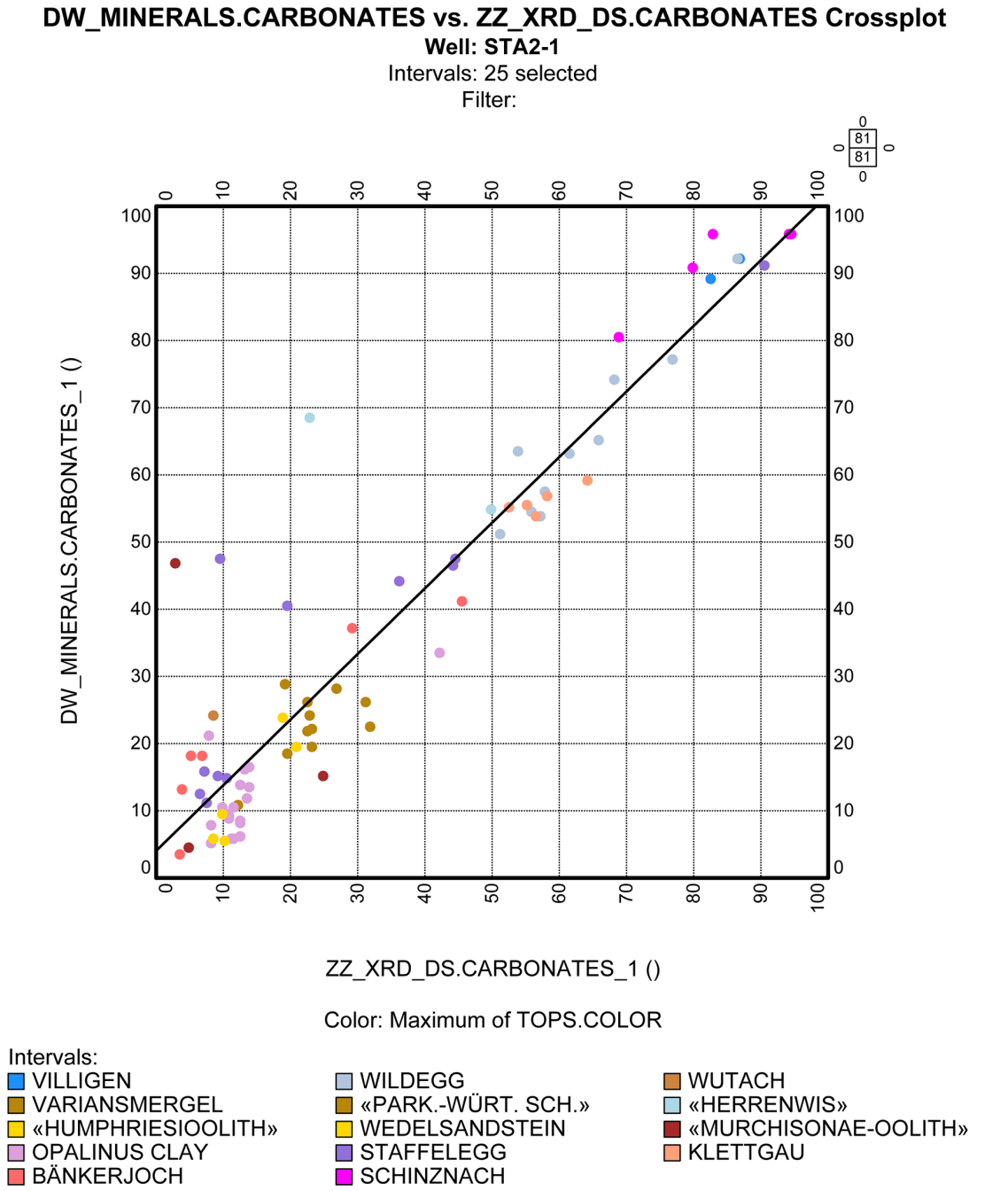

Fig. 4-5: Weight-% of carbonates (y-axis) compared to core XRD data (x-axis), Villigen to Schinznach Formation

The carbonates include the calcite, dolomite and siderite content. The calibration to core XRD data is good (cc = 0.94), despite a few outliers and local heterogeneities.

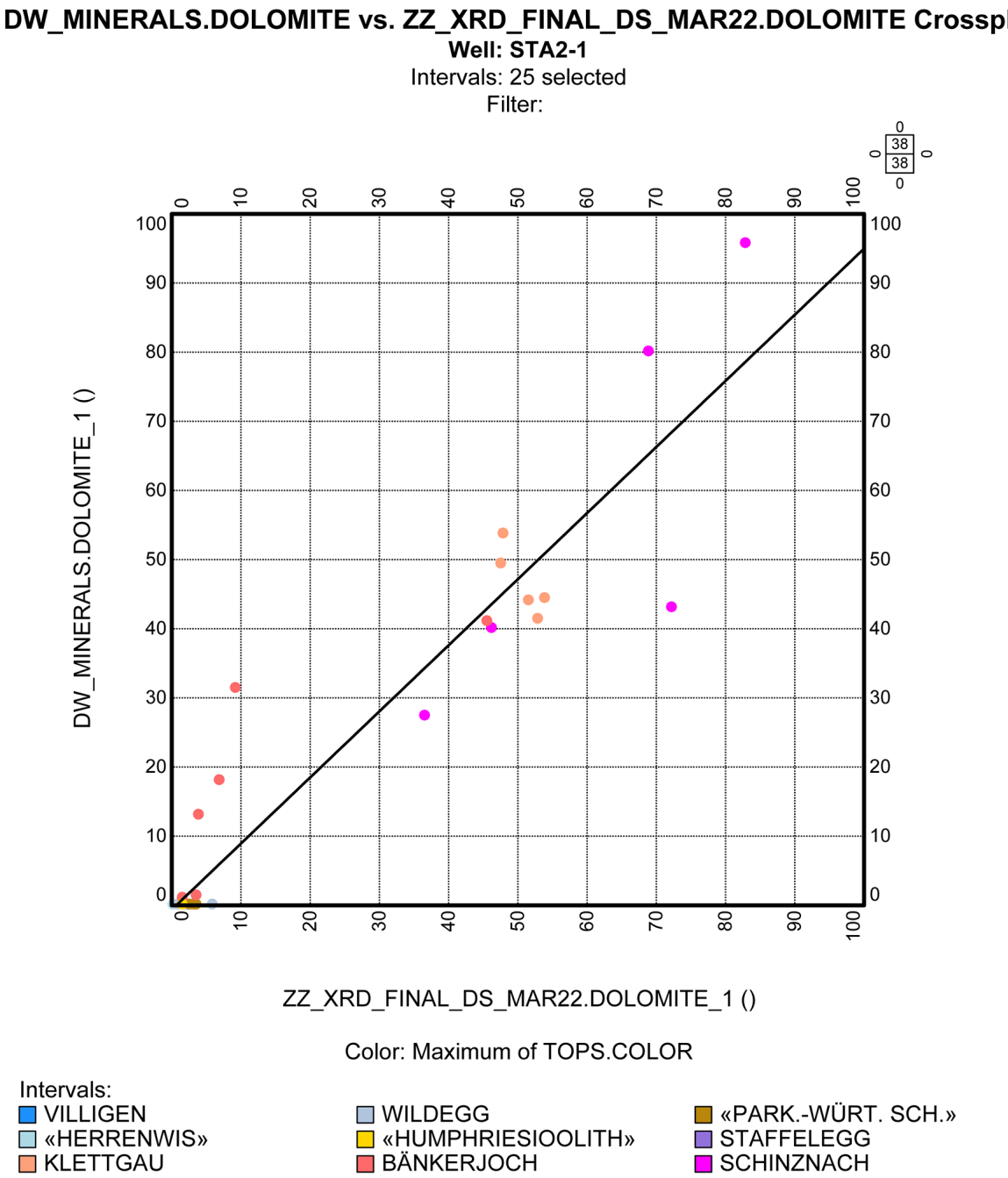

Fig. 4-6: Weight-% of dolomite (y-axis) compared to core XRD data (x-axis), Villigen to Schinznach Formation

The dolomites are mostly located in the Triassic, within complex mineralogical settings including anhydrite. The calibration to core XRD data is good (cc = 0.95) although some dispersion can be noticed.

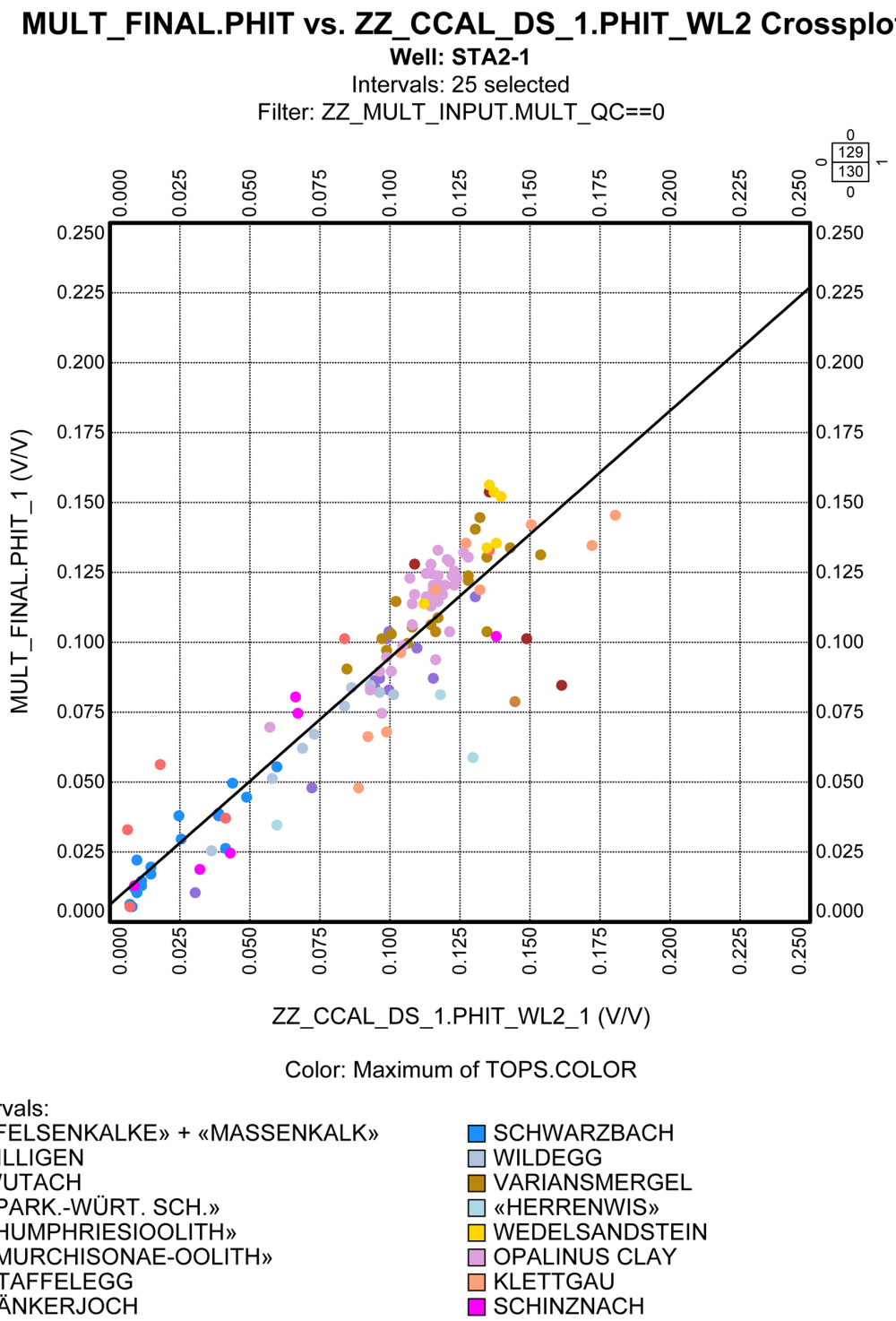

Fig. 4-7: Total porosity (v/v, y-axis) compared to core data (x-axis), «Felsenkalke» + «Massenkalk» to Schinznach Formation

The lab porosity used for the comparison was water-loss porosity (105 °C) using grain density, at ambient conditions, i.e. no confining stress was applied during measurements. Therefore, core and log measurements are not fully equivalent as the logs evaluate in situ wet formations. Nevertheless, the correlation between MultiMin and lab porosity is good (cc = 0.92).

MultiMin porosity is often close to core porosity, with some remaining dispersion likely related to local heterogeneities (core and logs measure at a different scale) and depth shift uncertainties.

4.2 Main results of the core-calibrated log analyses in the STA2-1 borehole

The main aim of the MultiMin interpretation were continuous curves of porosity and clay content of STA2-1. Several other minerals have been determined (mainly QF-silicates and carbonates). Below is a summary of the main parameters of clay, carbonate, QF-silicate content and porosity for each system/group.

If not stated otherwise, the clay content is used sensu lato meaning that the clay content is used as a general term for the total clay mineral content of the formation (i.e. the sum of all clay minerals). Carbonates and QF-silicates are also used sensu lato where carbonates are regarded as the sum of all carbonate minerals (calcite, dolomite and siderite) while QF-silicates are used synonymously for the sum of quartz (sensu stricto) and feldspars.

Malm (433.0 – 728.2 m, «Felsenkalke» + «Massenkalk», Schwarzbach Formation, Villigen Formation and Wildegg Formation)

As the 13⅜" auxiliary casing shoe was installed at 466.0 m MD (drillers depth), the top part of the Malm could not be logged (first valid wireline data at 470.5 m MD).

As expected, carbonates are the main constituents in the formations of the Malm, the mean calcite content is 85.1 wt.-% (median of 91.5 wt.-%). Lithological changes (e.g. at group boundaries) are sometimes reflected in a sharp negative peak (e.g. decreasing carbonate content at top Schwarzbach Formation and top Wildegg Formation correlated to clay content increase), but in general variance of the carbonates in the Malm is low.

Correlated to this high calcite content, the dry clay content is low (mean of 9.7 wt.-%, median of 5.6 wt.-%) with locally higher values in the more argillaceous intervals (e.g. parts of the Schwarzbach or Wildegg Formations). In the Wildegg Formation, the maximum clay content is close to 47.0 wt.-% with a mean and median of 20.7 and 20.9 wt.-%. The carbonate content in the Malm is dominated by calcite, as no dolomite was calculated for this group (up to 5.74 wt.-% on core XRD data in the Wildegg). No siderite was measured on core XRD.

The QF-silicate content in the Malm is low (mean of 4.8 wt.-%, median of 2.7 wt.-%). The more clay-rich lithologies (Schwarzbach Formation and Wildegg Formation) show a slightly increased QF-silicate content (mean / median of the Schwarzbach Formation: 6.2 / 5.9 wt.-%, Wildegg Formation: 10.7 / 10.3 wt.-%).

Total porosity in the Malm ranges between 0 and 13.5% (mean of 3.5%, median of 3.0% after applying the MULT_QC flag). The highest porosity is computed in the Wildegg Formation but must be treated with caution as it might represent artefacts due to reduced data quality in washout or breakout intervals.

Dogger (728.2 – 906.9 m, Wutach Formation, Variansmergel Formation, «Parkinsoni-Württembergica-Schichten», «Herrenwis Unit», «Humphriesioolith Formation», Wedelsandstein Formation, «Murchisonae-Oolith Formation», Opalinus Clay)

The boundary between the Malm and the Dogger is clearly marked by a sharp increase of the iron content (DWFE_ALKNA up to 26.5 wt.-%), by a thorium peak and a sharp decrease of the carbonate content to the Wutach Formation.

The carbonate content in the Dogger is generally moderate, with a mean of 20.7 wt.-% and a median of 12.5 wt.-%. The carbonate content is dominated by the calcite above the Opalinus Clay (mean / median 33.2 wt.-% / 28.3 wt.-%), and the calcite plus siderite in the Opalinus Clay (mean / median calcite 8.2 wt.-% / 6.5 wt.-%; mean / median siderite 2.9 wt.-% / 3.0 wt.-%). The dolomite content is low from XRD measurements (up to 4.73 wt.-% in the Variansmergel Formation), hence it could not be modelled.

The «Herrenwis Unit» has a high calcite content: maximum 88.3 wt.-%, mean of 76.5 wt.-% and median of 79.3 wt.-%.

Four calcite-rich thin streaks can be noticed in the upmost half of the Opalinus Clay, visible on the bulk density RHOZ and the calcium content DWCA_WALK2. These streaks are likely not well characterised due to the limited vertical resolution of the ECS tool.

The ECS iron content (DWFE_WALK2 and DWFE_ALKNA) show high values in the Dogger, mostly in the Wutach Formation and at the base of the «Murchisonae-Oolith Formation». The XRD analysis on core samples identified several iron minerals and locally high concentration of siderite (mostly in the Opalinus Clay), goethite (up to 38.6 wt.-% in the Wutach Formation) and some pyrite.

The QF-silicate content in the Dogger ranges between 0.0 and 49.1 wt.-%. The mean and median values (26.4 and 27.5 wt.-%) are increased in the Wedelsandstein Formation (mean / median 34.8 wt.-% / 33.3 wt.-%, maximum 49.1 wt.-%).

The Opalinus Clay at the base of the Dogger is certainly the formation with the highest clay content, ranging between 25.3 and 75.4 wt.-% (mean / median of 59.5 wt.-% / 62.8 wt.-%).

The clay content is high but variable in the formations above the Opalinus Clay (minimum 3.3 wt.-%, maximum 63.4 wt.-%, mean / median of 37.5 wt.-%).

Total porosity of the Dogger also is contrasted between the different units. PHIT is not very variable in the Opalinus Clay (minimum / maximum 5.3% / 13.6%, mean and median both 11.2% and 11.7% with a low standard deviation of 1.6%). It is more variable in the overlying Dogger formations (minimum / maximum 0.1% / 16.4%, mean / median 10.1% / 10.3% and a standard deviation of 3.5%). The maximum total porosity of 29.6% was measured on cores in the WutachFormation, in a goethite-rich layer but was not reconstructed by the MultiMin analysis (most likely because of poor log resolutions due to very thin layers).

Lias (906.9 – 941.4 m, Staffelegg Formation)

The formation boundary from the Opalinus Clay (Dogger) to the Staffelegg Formation (Lias) corresponds to a sharp drop of the clay content and a sharp rise of the carbonate (mostly calcite) content.

The carbonate content of the Lias varies between the different members. It is high in the upper part, Gross Wolf down to Grünschholz Members (maximum 80.4 wt.-%, mean / median 55.1 wt.-% / 55.9 wt.-%) and in the Beggingen Member (maximum 91.2 wt.-%, mean / median 73.5 wt.-% / 83.5 wt.-%). The Frick and Schambelen Members have a relatively lower carbonate content, respectively maximum 74.7 wt.-% and mean / median 15.4 wt.-% / 13.6 wt.-%, and maximum 52.9 wt.-% and mean / median 20.7 wt.-% / 19.5 wt.-%.

As in the previous groups, the carbonate content is dominated by calcite, a low dolomite content was measured on core (XRD up to 3.51 wt.-%). No siderite content was measured from cores, but some was computed in the Beggingen Member, driven by the high ECS iron content (DWFE_ALKNA up to 12.9 wt.-%).

The QF-silicate content is reversely correlated to the carbonate content. While the Gross Wolf down to Grünschholz Members and the Beggingen Member show a relatively low QF-silicate content (respectively mean / median 13.4 wt.-% / 13.2 wt.-% and 1.3 wt.-% / 0.7 wt.-%), the Frick and Schambelen Members show higher QF-silicate contents (respectively mean / median 35.7 wt.-% / 36.2 wt.-% and 16.6 wt.-% / 16.5 wt.-%).

The clay content follows a similar trend as the QF-silicates, moderate in Gross Wolf down to Grünschholz Members and the Beggingen Member (respectively mean / median 26.0 wt.-% / 27.3 wt.-% and 20.3 wt.-% / 6.5 wt.-%) and higher in the Frick and Schambelen Members (respectively mean / median 47.8 wt.-% / 47.5 wt.-% and 61.9 wt.-% / 63.5 wt.-%).

The Staffelegg Formation is also characterised by high total organic carbon (TOC), not fully reconstructed by the MultiMin interpretation with the available wireline logs. The maximum TOC measured on cores was 5.37 wt.-% at 917.47 m. This miscalibration of the TOC impacts the porosity computation.

The total porosity in the Staffelegg Formation ranges between 0.0 and 19.4 %, mean / median 8.1% / 8.3% (filtered for the MULT_QC flag).

Keuper (941.4 – 1'043.6 m, Klettgau Formation, Bänkerjoch Formation)

In the Keuper, the top part of the Klettgau Formation (Gruhalde to Gansingen Members) is characterised by a complex mineralogical mixture of carbonates (mostly dolomite) between 23.2 wt.-% and 82.9 wt.-%, mean / median 57.3 wt.-% / 55.3 wt.-%, silicates (quartz and feldspars) between 5.3 wt.-% and 37.3 wt.-%, mean / median 13.9 wt.-% / 12.4 wt.-%, and clays (dominant illite) between 2.3 wt.-% and 52.9 wt.-%, mean / median 28.4 wt.-% / 32.3 wt.-%.

The base Klettgau Formation (Ergolz Member) is an argillaceous, arkosic sandstone, up to 73.2 wt.-% QF-silicates, mean / median 55.1 wt.-% / 59.8 wt.-%. The clay content is 40.6 wt.-% mean and 39.3 wt.-% median.

The underlying Bänkerjoch Formation is dominated by anhydritic deposits: 0 to 96.6 wt.-% (mean 42.2 wt.-%). Carbonates (dolomite), clays and QF-silicates are well represented in this formation.

The total porosity in the Keuper ranges from 0 to 19.3% (mean 9.6% and median 10.2%). The lowest porosities correspond to the anhydrites, while the highest are located in the argillaceous layers.

Muschelkalk (1'043.6 – 1'225.1 m, Schinznach Formation, Zeglingen Formation, Kaiseraugst Formation)

The magnesium content was measured with the MGWALK closure model, which helped characterising the dolomite content of the Muschelkalk.

The boundary from the Keuper to the Muschelkalk is marked by a sharp increase of the carbonate content (which here is dolomite) and a correlated decrease of the anhydrite. The Asp and Stamberg Members are mostly dolomitic (except for a thin peak of QF-silicate and clay contents at the base of the Asp Member), while the top of the Liedertswil Member is a progressive transition to dolomitic limestones then limestones at the Leutschenberg/Kienberg Member bottom. The bottom part of the Leutschenberg/Kienberg Member is again a dolomitic limestone.

The carbonate content of the Schinznach Formation ranges from 0.0 wt.-% to 100 wt.-% (mean 90.2 wt.-%, median 94.2 wt.-%), this can be divided into a mean of 79.9 wt.-% dolomite in the Asp and Stamberg Members at the top, 34.2 wt.-% dolomite and 61.9 wt.-% calcite in the Liedertswil and Leutschenberg/Kienberg Members at base.

The top Zeglingen Formation is characterised by a sharp decrease of the calcite content, replaced by dolomite. The anhydrite content, well picked up by the ECS DWSU_WALK2 curve, increases downwards in the Dolomitzone Member, while the Sulfatzone Member is mostly anhydritic below 1'134.2 m.

The «Salzlager» is an intercalation of halite and anhydrite beds with a low clay content. Some washouts are observed in front of the halite beds, affecting the log quality. The Untere Sulfatzone Member is again mostly anhydritic.

A sharp anhydrite to carbonates and clays transition is observed 1 m below the top Kaiseraugst Formation, with a complex mineralogical mixture of carbonates, QF-silicates and clays: mean 28.5 wt.-% carbonates, 27.1 wt.-% QF-silicates and 37.9 wt.-% clays. A thin anhydritic bed is seen at base Orbicularismergel Member. The Wellendolomit Member shows a higher QF-silicate content, up to 68.4 wt.-%: mean / median 44.5 wt.-% / 40.3 wt.-%.

Total porosity in the Muschelkalk is very variable and ranges between 0 and 20.0%. The highest value is located within the dolomites of the Stamberg Member at the top Schinznach Formation.

The lowest porosity rocks are the halite beds, anhydrites and the dolomitic limestones in the Liedertswil and Leutschenberg/Kienberg Members at the base Schinznach Formation.

Buntsandstein (1'225.1 – 1'237.9 m, Dinkelberg Formation)

The boundary from the Muschelkalk to the sandstones of the Buntsandstein is characterised by a sharp increase of the QF-silicate content and a sharp decrease of the carbonate and clay contents. On the logs this corresponds to a gamma ray decrease.

The QF-silicate content is high in the Buntsandstein (mean / median of 89.5 wt.-% /92.7 wt.-%, maximum 98.9 wt.-%). The carbonate content is low, mean 6.0 wt.-% and median 3.9 wt.-%.

The clay content in the Buntsandstein is also low (mean / median: 4.5 wt.-% / 2.5 wt.-%, maximum 23.8 wt.-%).

Total porosity in the Buntsandstein ranges from 2.6% to 14.7% (mean 10.6%, median 11.8%).

Rotliegend (1'237.9 – 1'288.1 m, Weitenau Formation)

The MultiMin analysis could be run down to 1'284.9 m in the Weitenau Formation.

The main Weitenau Formation lithology is an argillaceous, arkosic sandstone, the QF-silicate content is high (mean / median: 61.2 wt.-% / 65.1 wt.-%, maximum 91.9 wt.-%).

The carbonate content in the Weitenau Formation is low (mean/median 3.0 wt.-% / 2.7 wt.-%,).

The clay content is moderate to high in the Rotliegend (mean/median: 35.8 wt.-% / 32.0 wt.-%, maximum 66.7 wt.-%).

The Weitenau Formation is a low porosity formation: 2.4% to 10.0%, mean/median 5.1 / 5.2%.

4.3 Main results of the core-calibrated log analysis in the Opalinus Clay (800.67 – 906.87 m)

The main results in terms of total clay content, mineralogy and total porosity for the main focus interval (Opalinus Clay) are shortly described in this section. Figs. 4-8 to 4-14 show some general statistical values of the MultiMin analysis results within the Opalinus Clay.

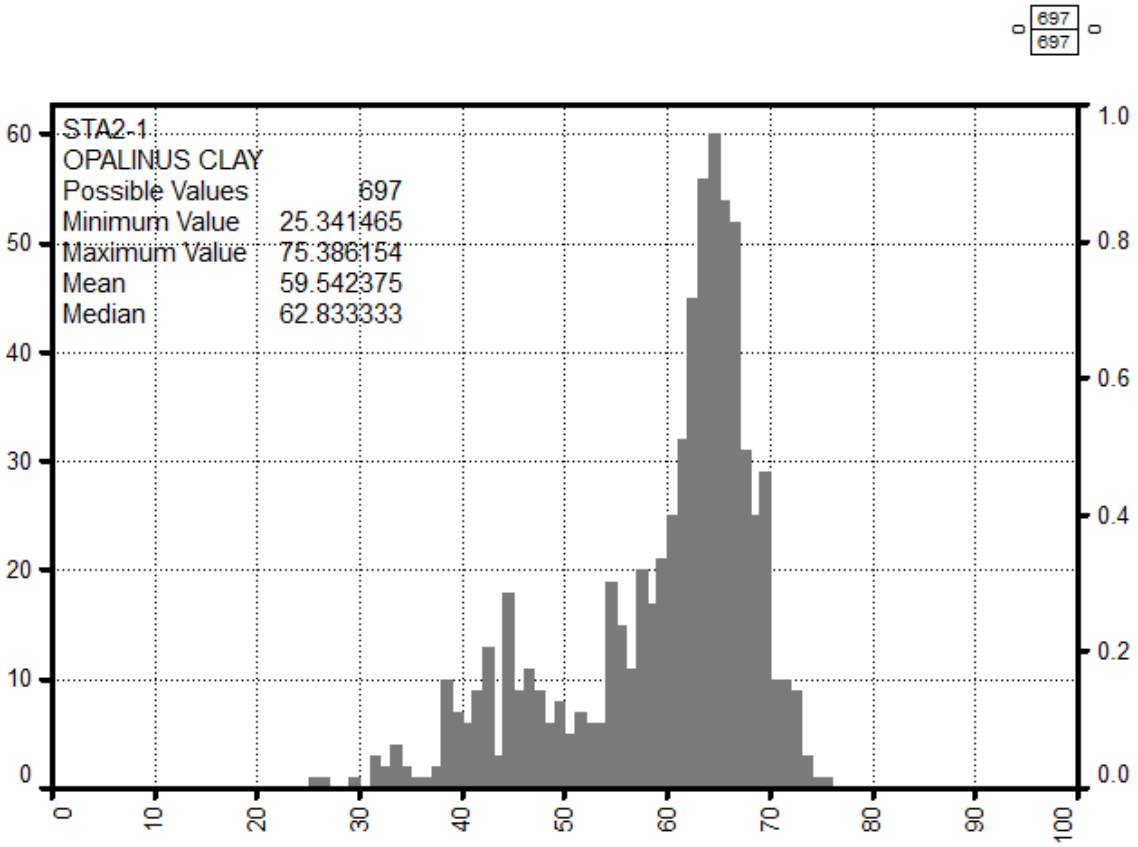

Fig. 4-8: Dry clay weight percentage frequency histogram in the Opalinus Clay

X-axis is the dry clay wt.-% from MultiMin, y-axis the number of points per bin (100 bins).

In the clay-rich Opalinus Clay, the mean and median dry clay contents are close to 59.5 wt.-% and 62.8 wt.-%. The distribution looks bimodal, with the lowest clay content in the shallowest part of the Opalinus Clay.

The two next frequency histograms (Figs. 4-9 and 4-10) show a split of the Opalinus Clay into an upper and lower part, showing that the latter is slightly more argillaceous.

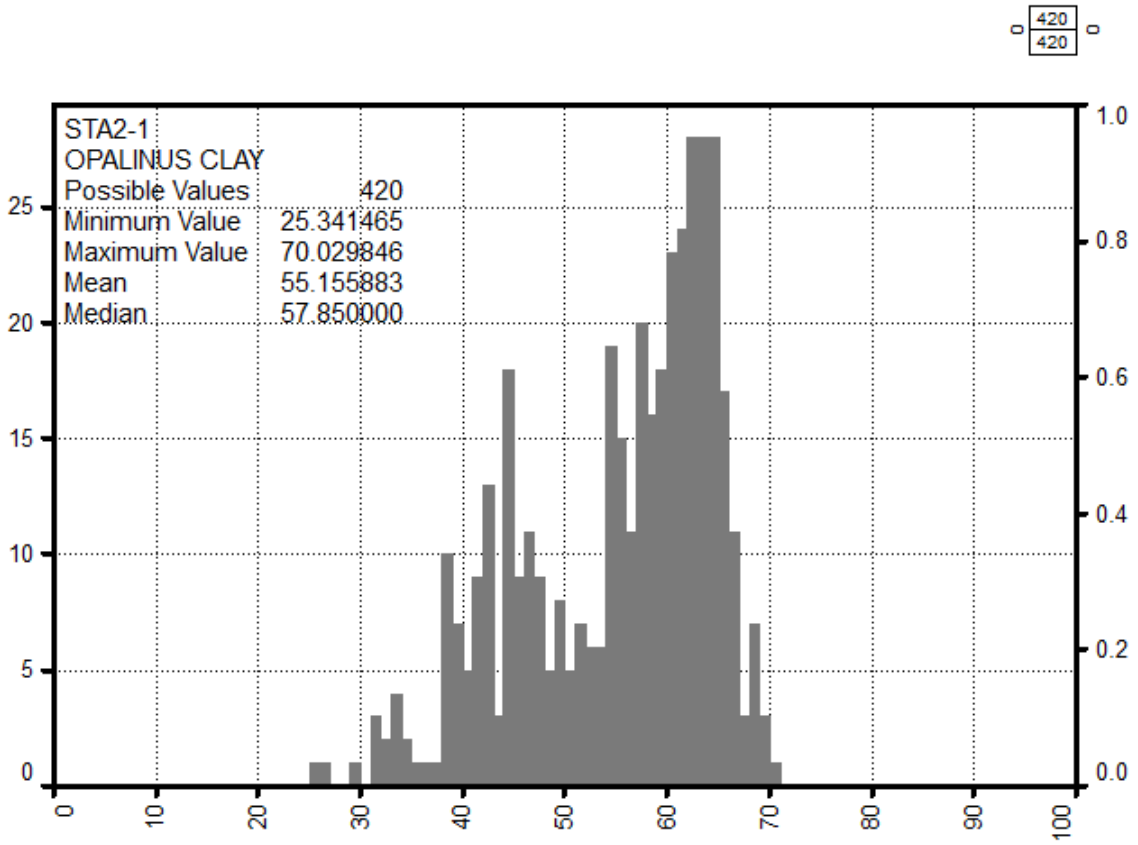

Fig. 4-9: Dry clay weight percentage frequency histogram in the upper section of the Opalinus Clay (above 864.7 m)

X-axis is the dry clay wt.-% from MultiMin, y-axis the number of points per bin (100 bins).

In the upper part of the Opalinus Clay (above 864.7 m), the mean and median dry clay contents are close to 55.2 wt.-% and 57.9 wt.-%. The top part of the formation is significantly less argillaceous than the bottom, see Fig. 4-10.

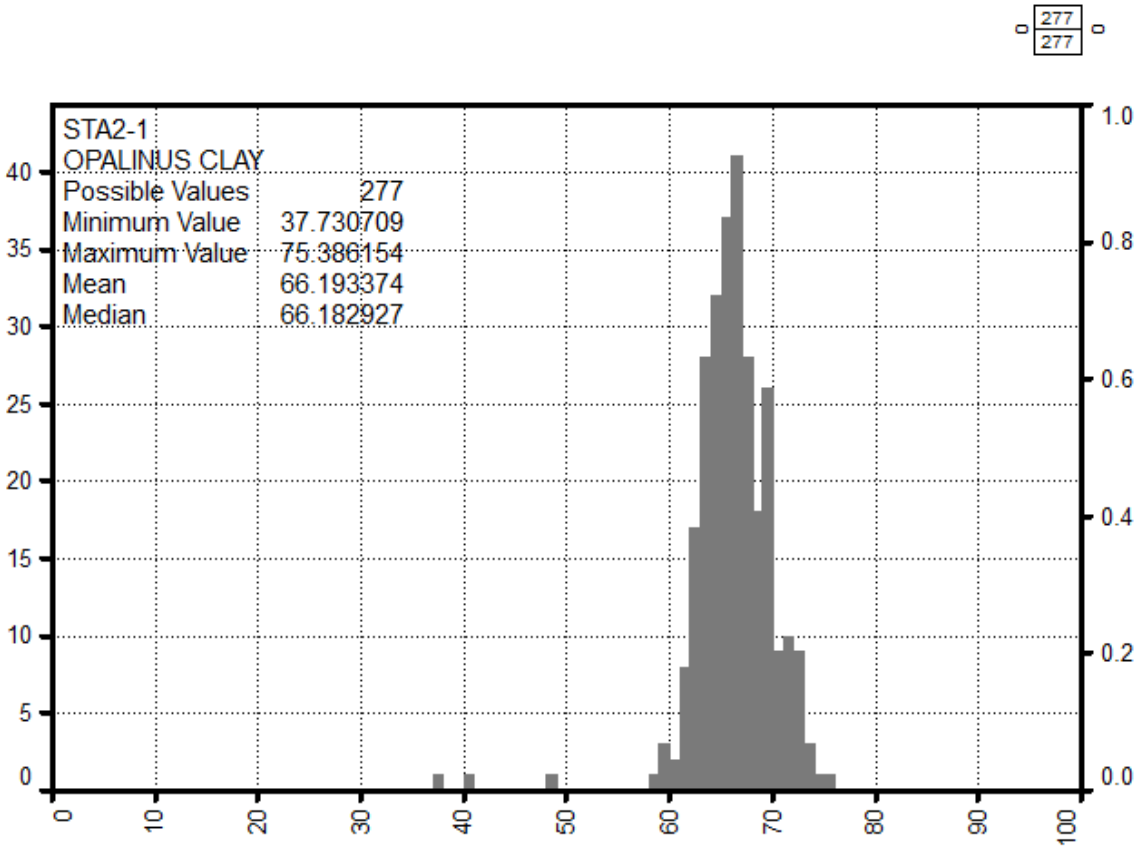

Fig. 4-10: Dry clay weight percentage frequency histogram in the lower section of the Opalinus Clay (below 864.7 m)

X-axis is the dry clay wt.-% from MultiMin, y-axis the number of points per bin (100 bins).

The bottom part of the Opalinus Clay (below 864.7 m) is more argillaceous: the mean and median dry clay contents are close to 66.2 wt.-%.

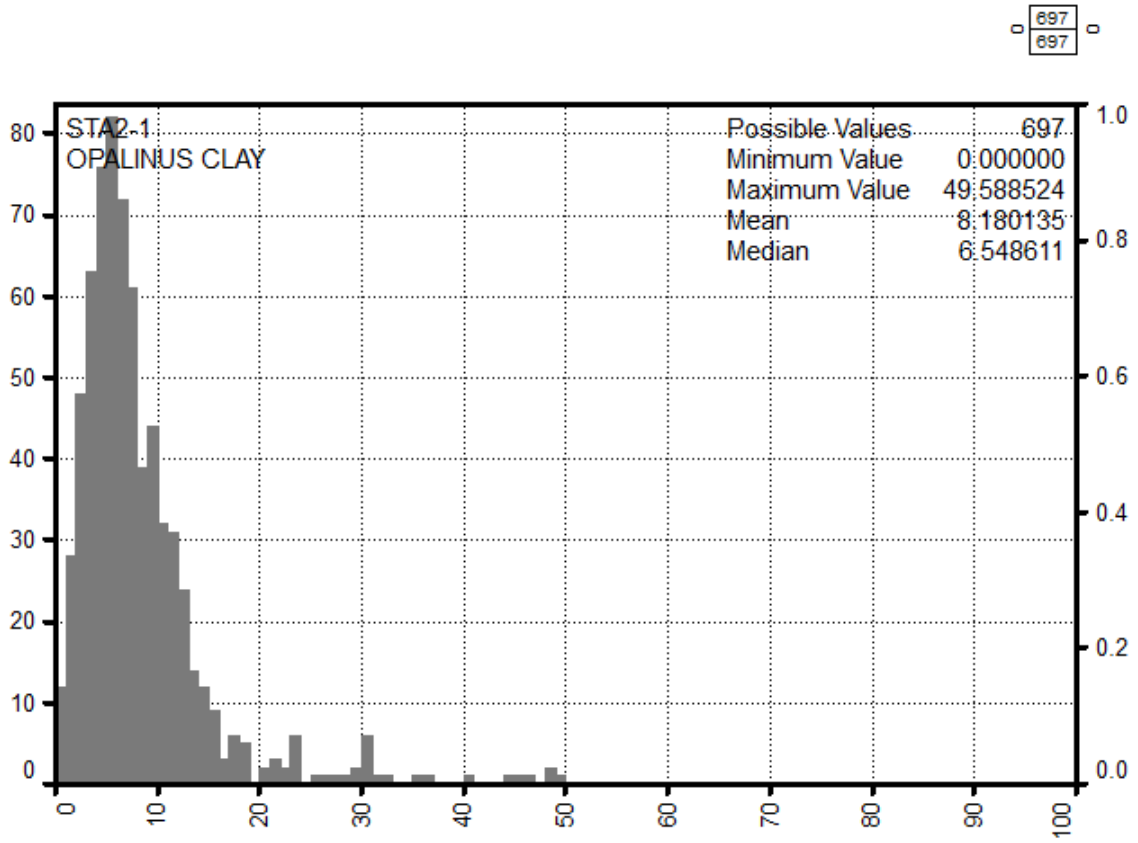

Fig. 4-11: Calcite weight percentage frequency histogram in the Opalinus Clay

X-axis is the calcite wt.-% from MultiMin, y-axis the number of points per bin (100 bins).

The mean and median calcite contents are close to 8.2 wt.-% and 6.5 wt.-% (Fig. 4-11). The maximum values are up to 49.6 wt.-%, i.e., corresponding to thin, calcite-rich layers. In case these layers are thinner than the log resolution, the maximum calcite content would be higher than computed by MultiMin.

The top part of the Opalinus Clay is more calcitic than the bottom, see Plates 1 and 2.

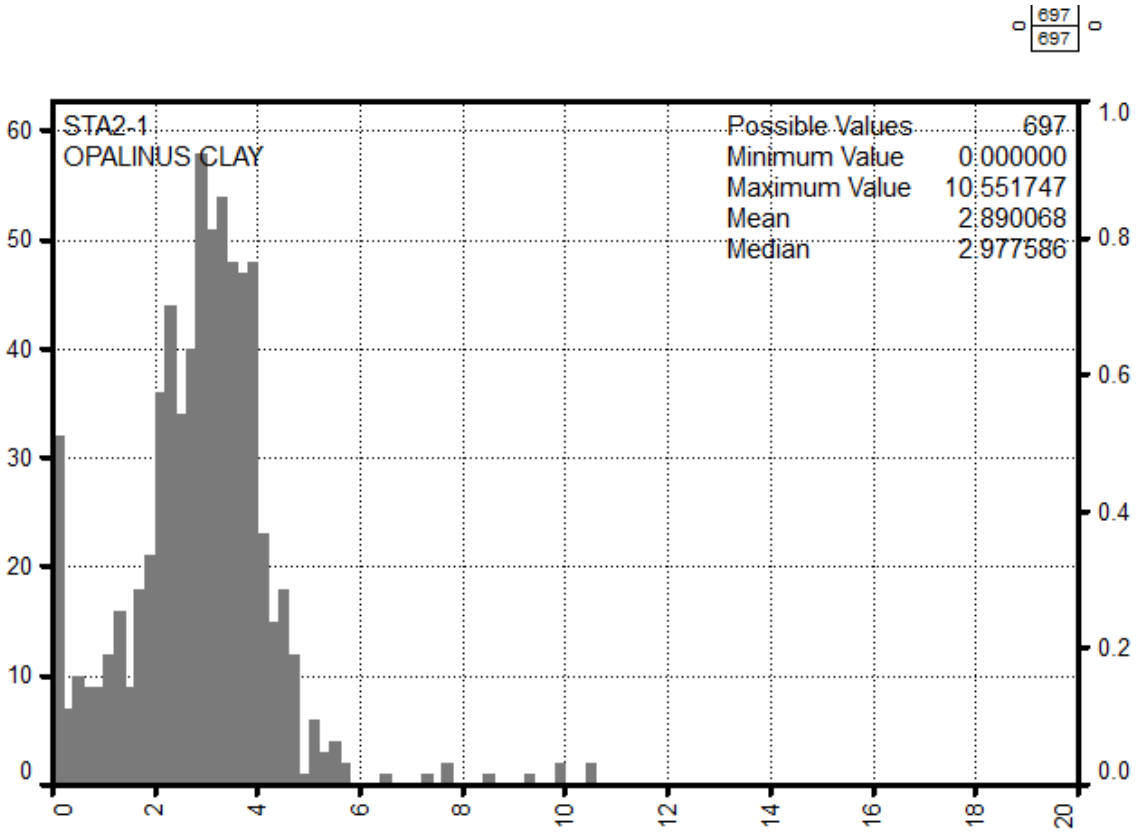

Fig. 4-12: Siderite weight percentage frequency histogram in the Opalinus Clay

X-axis is the siderite wt.-% from MultiMin, y-axis the number of points per bin (100 bins).

The mean and median siderite contents are close to 2.9 wt.-% and 3.0 wt.-%, with a maximum value of 10.6 wt.-% and minimum values close to 0 wt.-% (Fig. 4-12). Please note that the siderite core calibration is less constrained than other minerals.

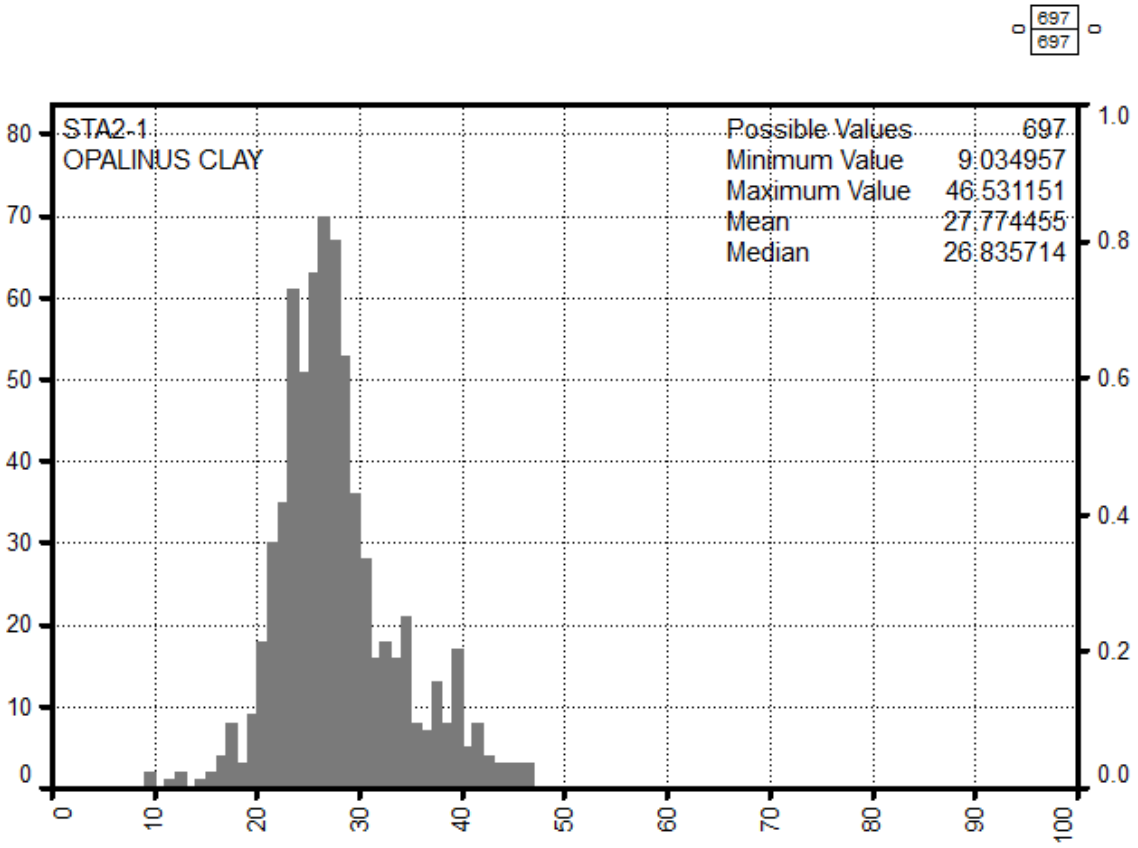

Fig. 4-13: QF-silicates (quartz and feldspars) weight percentage frequency histogram in the Opalinus Clay

X-axis is the QF-silicates wt.-% from MultiMin, y-axis the number of points per bin (100 bins).

The mean and median QF-silicates (quartz, plagioclases and potassic feldspars) contents are close to 27.8 and 26.8 wt.-% (Fig. 4-13), much higher than the carbonates (calcite close to 8 wt.-%).

From core XRD data, the quartz represents two thirds and feldspars the remaining third of the total QF-silicate content.

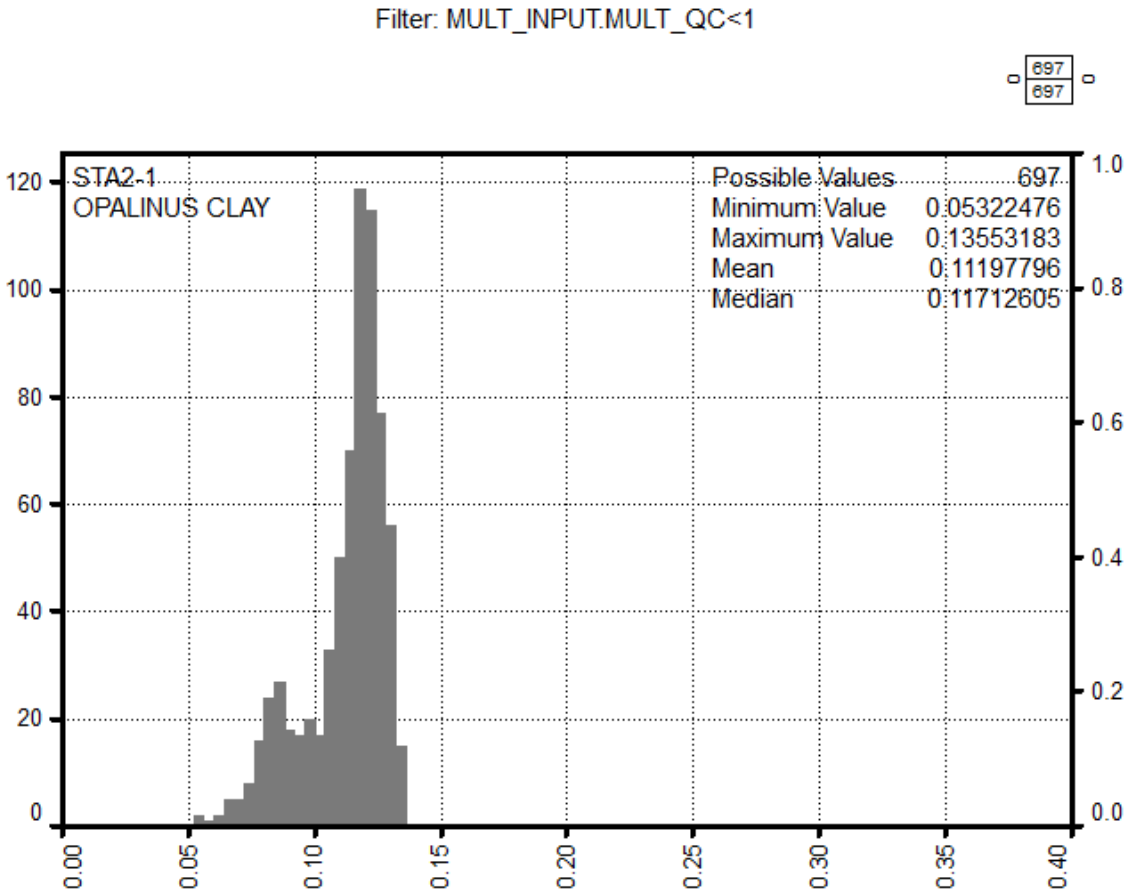

Fig. 4-14: Total porosity frequency histogram in the Opalinus Clay

X-axis is the total porosity v/v from MultiMin, y-axis the number of points per bin (100 bins).

The mean and median total porosities are close to 11.2% and 11.7%, with a range from 5.3% to 13.6% (Fig. 4-14). The distribution is bimodal, reflecting the distribution of the clay content.

Fig. 4-15 summarises the main results in the Opalinus Clay.

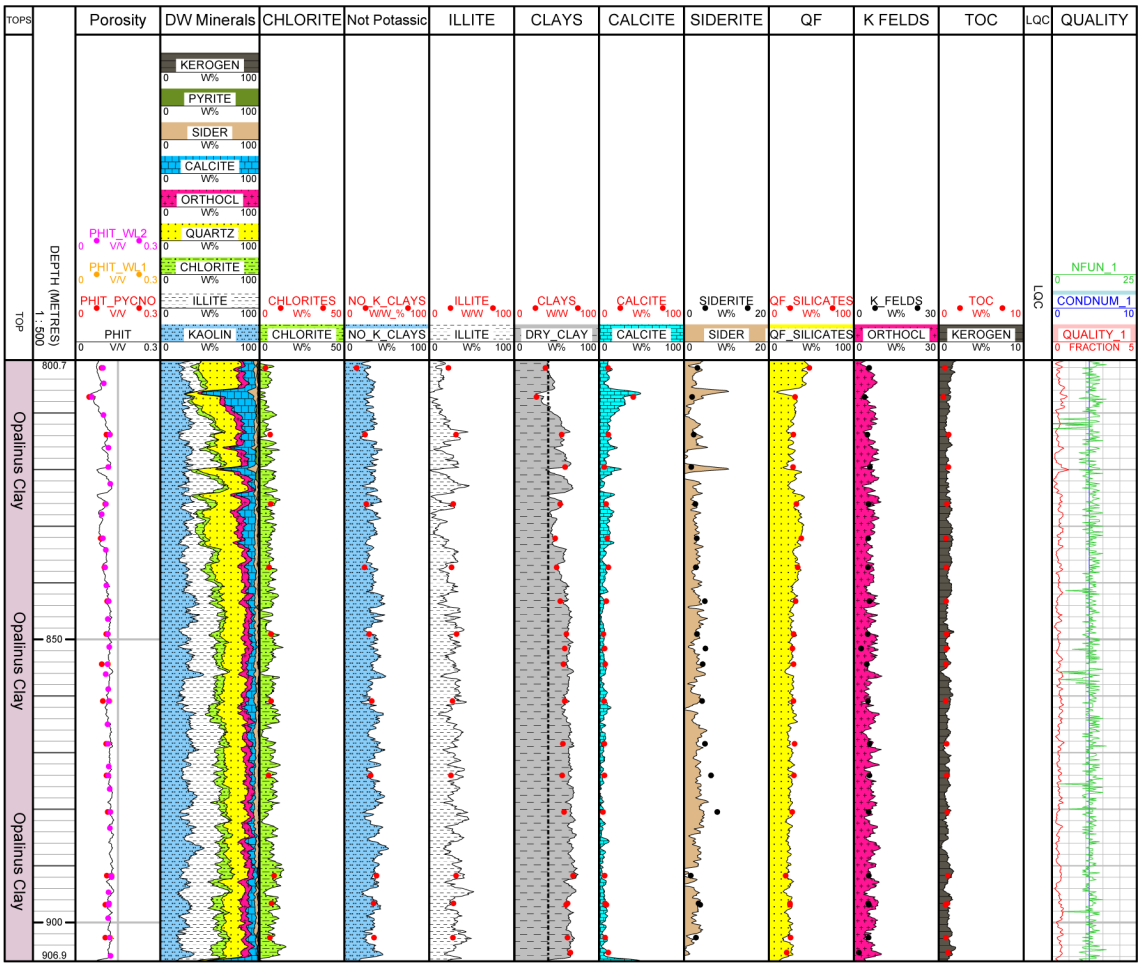

Fig. 4-15: Main log and core results in the Opalinus Clay

The dashed back line in the Clays track represents a 40% baseline.

The wireline log quality was good in all the Opalinus Clay, as shown by the green LQC flag.

The MultiMin quality curve always remains low, generally below 1.00, indicating an overall good curve prediction.

The total porosity and the main minerals dry weight are well calibrated to the core XRD measurements. The siderite, illite and TOC calibrations are less accurate.

The whole Opalinus Clay is very argillaceous, almost always above the 40 wt.-% (black line in the "Clays" track in Fig. 4-15). A few carbonates streaks in the top part have a lower clay content.

5 Summary

The MultiMin interpretation was successfully applied in the STA2-1 borehole using the Paradigm Geolog MultiMin software (see Plates 1 and 2). Based on available petrophysical logs and formation mineralogical contents, several specific MultiMin interpretation intervals were identified. Some of these intervals needed to be further subdivided due to e.g. borehole conditions to ensure the best possible MultiMin interpretation result.

Core data from lab measurements were also available so that the mineralogical content and other parameters (e.g. density and/or porosity) were known at several points along the borehole. These core data included bulk rock XRD mineralogy, clay mineralogy, pycnometer and water loss porosity as well as grain density. The core data was used as a calibration dataset for the MultiMin interpretation where available.

The mineralogical MultiMin interpretation results were converted to weight percentages for a straightforward comparison with core XRD measurements. In general, the comparisons showed a good agreement between the mineralogy (and porosity) from the MultiMin interpretation and the core data, despite some remaining uncertainty on the core to log depth shift. QF-silicates and carbonates show a good agreement with core data throughout the borehole even in the lowermost units. The differentiation between illite (potassic clay), non-potassic clays and chlorite end-members was not very well achieved. The total porosity is well calibrated to core measurements in the Opalinus Clay; the calibration was good in the whole borehole, with remaining dispersion possibly related to depth shift uncertainties and rock heterogeneity. The recent quantification of goethite from the core XRD data allows a better evaluation of the iron-rich formations of the Dogger.

The continuous curves from the MultiMin interpretation can be used to characterise the different formations (and hence members) occurring in STA2-1. The Opalinus Clay shows a quite variable total clay content though in most locations it is well above 40 wt.-%, except in the uppermost 33 m. The lower part of the formation is significantly more argillaceous than the top, as already noticed in many regional locations.

In addition, boundaries between formations (and between members) are often clearly marked by a decrease or increase of clay, QF-silicate and/or carbonate contents. The carbonate-rich formations can further be characterised according to the occurrence of dolomite (replacing calcite), especially in the lower part of the borehole (in the lithostratigraphic units of the Keuper and Muschelkalk). The recent measurement of the magnesium content with the ECS tool (MGWALK closure model) greatly supported the calcite – dolomite characterisation in these formations. Similarly, the aluminium quantification with the ECS ALKNA closure model supported the clay content evaluation in the Malm and Dogger.

6 References

Isler, A., Pasquier, F. & Huber, M. (1984): Geologische Karte der zentralen Nordschweiz 1:100'000. Herausgegeben von der Nagra und der Schweiz. Geol. Komm.

Marnat, S. & Becker, J.K. (2021): Petrophysical log analyses of deep and shallow boreholes: Methodology report. Nagra Arbeitsbericht NAB 20-30.

Mazurek, M. (2017): Gesteinsparameter-Datenbank Nordschweiz – Version 2. Nagra Arbeitsbericht NAB 17-56.

Nagra (2014): SGT Etappe 2: Vorschlag weiter zu untersuchender geologischer Standortgebiete mit zugehörigen Standortarealen für die Oberflächenanlage. Geologische Grundlagen. Dossier II: Sedimentologische und tektonische Verhältnisse. Nagra Technischer Bericht NTB 14-02.

Pietsch, J. & Jordan, P. (2014): Digitales Höhenmodell Basis Quartär der Nordschweiz – Version 2013 (SGT E2) und ausgewählte Auswertungen. Nagra Arbeitsbericht NAB 14-02.

Waber, H.N. (ed.) (2020): SGT-E3 deep drilling campaign (TBO): Experiment procedures and analytical methods at RWI, University of Bern (Version 1.0, April 2020). Nagra Arbeitsbericht NAB 20-13.